UNIVERSIDADE FEDERAL DO ABC
CENTRO DE ENGENHARIA, MODELAGEM E CIÊNCIAS SOCIAIS APLICADAS
PROGRAMA DE PÓS-GRADUAÇÃO EM ENGENHARIA MECÂNICA

Kemron Beache

ACTIVE VIBRATION CONTROL OF A SMART BEAM UNDER ROTATION

Santo André / SP
June 28, 2016

Kemron Beache

ACTIVE VIBRATION CONTROL OF A SMART BEAM UNDER ROTATION:

Dissertação de mestrado apresentada ao Programa de Pós-Graduação em Engenharia Mecânica da Universidade Federal do ABC como parte dos requisitos para a obtenção do título de Mestre em Engenharia Mecânica.

Área de concentração: Mecânica dos Sólidos / Dinâmica de Sistemas

Orientador: Andre Fenili

Santo André / SP

June 28, 2016

DEDICATÓRIA

Dedico este trabalho aos meus pais e para as pessoas de Saint Vincent and the Grenadines, em especial pela dedicação e apoio em todos os momentos difíceis.

AGRADECIMENTOS

Ao Programa de Pós-Graduação em Engenharia Mecânica, POSMEC, pela oportunidade de realização de trabalhos em minha área de pesquisa.

Aos colegas do POSMEC pelo seu auxílio nas tarefas desenvolvidas durante o curso e apoio na revisão deste trabalho.

À CAPES provisão da bolsa de mestrado.

RESUMO

Uma viga em rotação é equipada com sensores e atuadores piezoelétricos em conjunto com um controlador proporcional-derivativo (PD) ou um controlador do tipo regulador linear quadrático (LQR) para comparação. O objetivo dos controladores é a minimização da deflexão na extremidade livre da estrutura devido ao seu movimento em torno do eixo de rotação. Utilizando o efeito piezoelétrico – a geração de uma voltagem quando a estrutura está sujeita a uma tensão mecânica – e, inversamente, a geração de uma deformação quando sujeito a uma voltagem, a estrutura do tipo viga é considerada como um sistema inteligente, tendo a capacidade de detectar e corrigir deflexões ao longo de seu comprimento. Usando as equações de Lagrange, a equação governante do movimento é obtida para a viga. A força (momento) e a rigidez da cerâmica piezoelétrica são subsequentemente adicionadas à equação governante da viga. A função de Heaviside é usada para a localização do atuador piezoelétrico ao longo da viga. A posição do atuador piezoelétrico varia a partir da extremidade engastada até a extremidade livre da viga ocupando três diferentes posições. O comprimento do atuador piezoelétrico é de um terço do comprimento da viga. O melhor posicionamento do piezoelétrico dentre os investigados é determinado para os três primeiros modos de vibração. Duas técnicas de controle linear são investigadas com o objetivo de eliminar a vibração na estrutura flexível: PD e LQR. O grau de liberdade associado ao movimento de rotação da viga (e suas derivadas) é prescrito por meio de um perfil pré-definido.

Palavras-chave: sensor piezoelétrico, atuador piezoelétrico, controle ativo de vibração, PD, LQR.

ABSTRACT

A rotating beam is fitted with piezoelectric sensors and actuators in conjunction with a proportional-derivative (PD) controller and a linear quadratic regulator (LQR) controller in order to minimize the deflection of the tip due to the rotational motion of the structure. Utilizing the piezo effects, the generation of a voltage, when subjected to a strain, and conversely the generation of a strain when subjected to a voltage, the system is considered as smart, having the ability to sense and correct deflections of the tip of the beam. Using the equations of Lagrange, the governing equation of motion is derived for the beam. The force (moment) and the stiffness of the piezo ceramic are subsequently added to the governing equation of the beam. In a model of the system, a Heaviside function is used to manipulate the position of the piezo. The position of the piezo will be varied from the root of the beam (the clamped end) to the free end of the beam, occupying three different positions; the length of the piezo is a third of the beam's length. The best position of the piezo is determined for three modes of vibration. Two linear control techniques are investigated in order to eliminate vibration in the flexible structure. The degree of freedom associated with the rotational motion is obtained by a predefined profile.

Keywords: piezoelectric sensor, piezoelectric actuator, active vibration control, PD, LQR.

TABLE OF CONTENTS

CHAPTER 1

Introduction

Light weight and flexible structures have many benefits. They are aesthetically appealing, less weight normally translates to lower energy consumption and increased performance, and they are easily deployed and assembled. Light weight structures should be defined as structures where the ratio of their mass to their length is relatively low. However, light weight and flexible structures present the challenge of maintaining stability because of their susceptibility to long vibration decays. Many parts of these structures can be modelled as simple beams.

Long, slender objects are traditionally modelled as Euler-Bernoulli beams, while short, fat objects modelled as Timoshenko beams, which take in account shear deformation. Here we are investigating an Euler-Bernoulli beam, undergoing rotation, and subject to vibration; hence, only axial stresses will be taken into consideration, and rotational inertia would not be consider. The purpose of this research is to investigate the use of piezoelectric material to minimise the displacement due to vibration. The investigation of using piezoelectric material in the control of vibration is vast. Finite element models such as (NARAYANAN & BALAMURUGAN, 2002) have been used to analyse the behaviour of a vibrating beam due to the introduction of a disturbing force with a piezo actuator and sensor acting to restore the beam to the desired position. In their analysis the effects of different control techniques, in particular, Constant-gain negative velocity feedback, Lyapunov feedback, and Linear quadratic regulator is explored, as well as the effects of temperature on the properties of the piezo material. The piezo is modelled as Timoshenko beam, applying Timoshenko shear flexible beam theory. However, here the assumed modes method will be used for developing the initial governing equation, and later deriving the modal stiffness and force from the piezo, which is to be added to the final governing equation. The vibration will be the result of

motion of the beam. The piezo material can be used at a single location or multiple as considered by (MOLTER, FONSECA, & BOTTEGA, 2009). Using the Heaviside function the location of the piezo is varied in order to observe the effects. In (MOLTER, FONSECA, & BOTTEGA, 2009) the authors state from other references that the first mode of vibration is the most important, and it is most effectively controlled by the placement of the piezo starting at the root of the beam. This result similar to (ABREU, RIBEIRO, & STEFFEN JÚNIOR, 2003), where a cost function was developed as to determine the optimal placement of the piezo actuator and sensor. The higher the value of cost function for a given configuration, the more control is shown by the sensor and actuator in controlling a mode. The highest value of the cost function was obtained when the piezo sensor and actuator started at the $x = 0.00\ m$ position. An optimal position will not be derived here; the piezo is to be varied at three locations: the root, middle, and end, with the length of the piezo being a third of the beam. This is a similar concept to what was employed by (GANI, SALAMI-SMIEEE, & KHAN, 2003), who similarly to (NARAYANAN & BALAMURUGAN, 2002), used a finite elements modeling. The beam was fitted with a piezo actuator and sensor a third of its length, with one end of the beam fixed and the other free with the presence of a disturbing force. The first and second modes of vibration were considered, and from the results, the most effective position of the piezo was shown to be at the root of the beam, concurrent with most other research.

The piezoelectric ceramic is a type of intelligent material due to the properties: direct and inverse piezoelectric effects; hence, it has the ability to be used as the sensor or actuator in active vibration control (ZHANG, HE, & WANG, 2010); however, care must be taken that the voltage supply to the piezo does not exceed the break down voltage: that is, the voltage at which the piezo material loses its ability to function as a smart martial. Two control techniques will be the used: a Proportional Differential control, applied by (SHUEEI-MUH, 2007), who demonstrated the effects of manipulating the Proportional and Differential gains on the frequencies and decay rates of the system; and the Liner quadratic regulator, applied in several other research papers.

Traditionally, the methods of controlling mechanical vibration fall into two classifications: Active and Passive controls. Passive methods involve the addition of some constant external force to act as a damper, or construction using more rigid materials. Many

light weight and flexible structures are employment in high performance and precision applications; hence, for optimal performance, it is required that they possess the ability to sensing and responding to changes in their environment. The use of the Piezoelectric ceramic adhered to the surface of the structure to counteract the effects of vibration will not add significant weight to the original structure and will not affect the initial flexibility characteristic.

1.1 Hypotheses

The tip deflection of a rotating beam due to vibration can be significantly reduced with the application of piezoelectric ceramics in conjunction with a control technique. The piezo ceramics applied on either side of the beam are to function in an actuator sensor relationship; hence, the system is deemed to be smart.

1.2 Objectives

The objectives of this dissertation are:

- Minimize the tip displacement of a rotating beam by integration piezoelectric ceramics along the length of the beam.

- Maintain the beam's flexibility and light weight.

- Have the ability to manipulate the position of the piezo in order to observe its effects on the behaviour of the beam, hence determining the best general position.

- Check applicability in three modes of vibration of this technique.

- Evaluate effectiveness of PD and LQR controllers in the control of tip displacement.

The system components are the beam under rotation of a proposed profile for theta Θ and the piezoelectric material, whose effect will be added as stiffness and moment force. The profile for theta Θ considered here can be consider as similar to the motion of a robotic arm moving through one quadrate of a circle and returning to its initial position; the profile can be changed to observe the beam's behaviour in different systems.

Here, the rotation is assumed to be taking place at slow speeds so that linear relationships may be applied.

The rotation profile is depicted in Figure 1.

The beam used in this work has the following characteristics: L (length) = 1.2m, E (young's modulus) = 0.7e11N/m2, ρ (density) = 2700kg/m^3, cross section: thickness = 0.0015 m, height = 0.02 m

The characteristics of the piezo actuator are: $E_a(P_a)$ young's modulus of the piezo, d_{31a} the piezo electric strain constant and $E_a d_{31a}$ the piezo actuation force and are given by:

$$E_a(P_a) = 71.4e9\frac{\mathrm{N}}{\mathrm{m2}},\ d_{31a} = 200e(-12)\left(\frac{m}{v}\right),\ E_a d_{31a} = 14280e(-3)\frac{N}{mv}$$

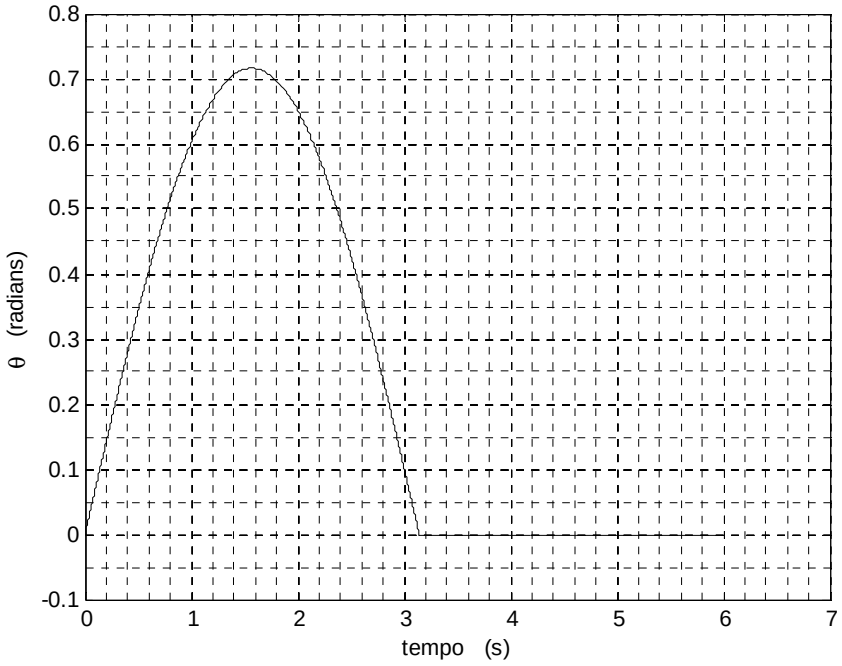

Figure 1.1 The prescribed profile for the angular displacement, theta.

CHAPER 2

Governing equation of motion for a rotating flexible beam

2.1 The Lagrange method

The governing equation of a flexible Euler-Bernoulli beam can be derived using Lagrange's equations (FENILI, 2000).

The Euler-Bernoulli beams are used here because:

- This beam model is ideal for modelling of long thin beam.
- The deflection of the beam is due to bending stress.
- It is the type of beam most utilized for modelling of flexible structures.
- Mathematical model of the beam (linear undamped and free from external efforts)

The equation of motion for a cantilever beam given is given by:

$$Elv^{iv}(x,t) + \rho A\ddot{v}(x,t) = Q \tag{2.1}$$

where: E is the Young's module, I is the moment of inertia of the beam cross section, ρ is the beam density, A is the cross section area, Q is the external force, and $v(x,t)$ is the transversal displacement of the beam.

2.2 The assumed modes method

The assumed modes method is utilized for the discretization a continuous function into discrete parts of space and time. The discretization variable is given as the following:

$$v(x,t) = \sum_{i=1}^{n} \emptyset_i(x) q_i\,(t) \tag{2.2}$$

where:

n represents the number of models to be adopted in discretization

$\emptyset_i(x)$ represents each one of the mode properties of the system

$q_i(t)$ are the states that are to be determined, or, the amplitudes of the modes

The functions $\emptyset_i(x)$ in Equation (2.2) are the solutions of the Euler-Bernoulli linear, undamped and unforced beam equation given by:

$$EIv^{iv}(x,t) + \rho A\ddot{v}(x,t) = 0 \tag{2.3}$$

An example for the shape functions, $\emptyset_i(x)$, for the clamped-free beam is as follows:

$$\emptyset_i(x) = \cosh(a_i x) - \cos(a_i x) - \alpha_i\big(senh(a_i x) - sen(a_i x)\big) \tag{2.4}$$

where:

$$\alpha_i = \frac{\cosh(a_i l)+\cos(a_i l)}{senh(a_i l)+sen(a_i l)} \tag{2.5}$$

and $a_i L$ are the eigenvalues associated to this system. The three eigenvalues for the first three modes of vibration are:

a_1L =1.878

a_2L = 4.6943

a_3L = 7.8548

The corresponding natural frequencies ($5.4\,\frac{\text{rad}}{\text{s}}$, $33.7\,\frac{\text{rad}}{\text{s}}$, and $94.5\ \frac{\text{rad}}{\text{s}}$) are given by:

$$w_i = (a_i L)^2 \sqrt{\frac{EI}{\rho A}} \tag{2.6}$$

2.3 Developing the governing equation of motion

The geometric model used in this work is depicted in Figures (1.2) and (1.3).

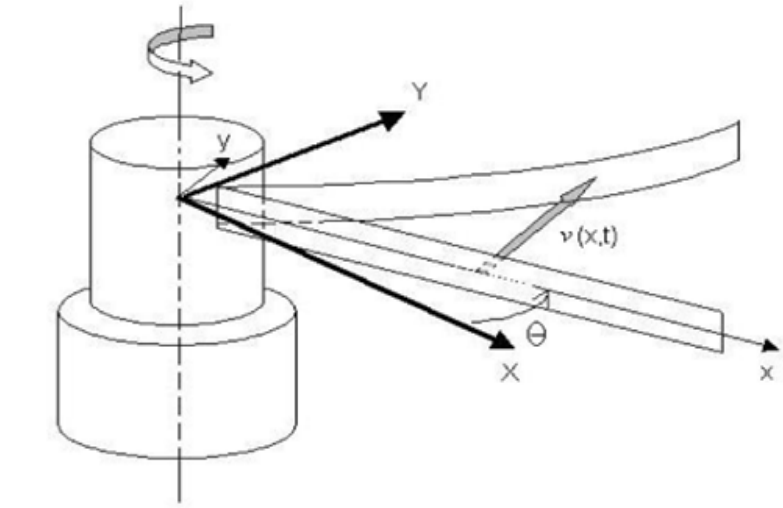

Figure1.2 A flexible beam rotating around a central hub.

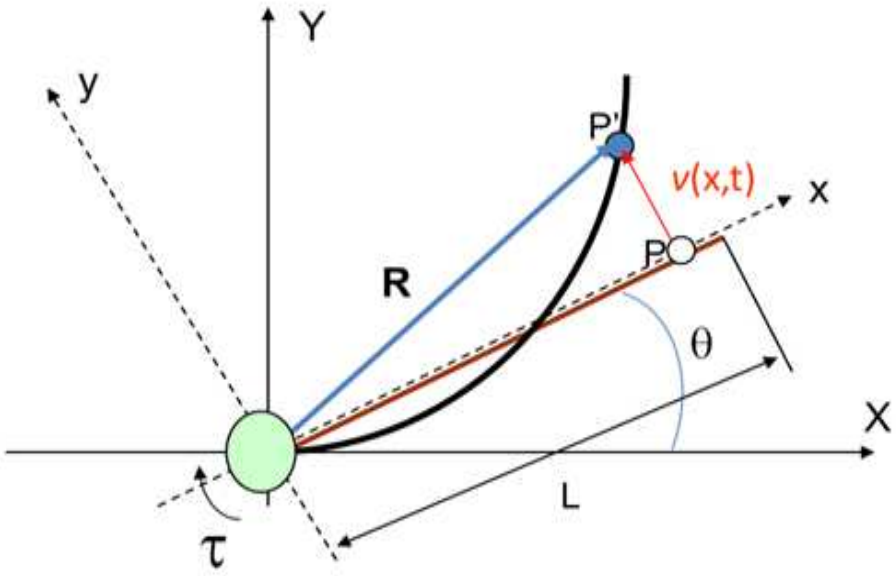

Figure 1.3 The vector displacement of a point long a rotating beam.

The vector position is obtained from the horizontal and vertical location of a point along the beam and using the geometric relationship between a fixed and rotating XY axis:

$$R = (xcos\theta - vsin\theta)i + (xsin\theta + vcos\theta)j \tag{2.7}$$

Taking the derivative of the vector position gives the vector velocity given by:

$$\dot{R} = \left(\dot{x}cos\theta - x\dot{\theta}sin\theta - \dot{v}sin\theta - v\dot{\theta}cos\theta\right)i + \left(\dot{x}sin\theta + x\dot{\theta}cos\theta + \dot{v}cos\theta - v\dot{\theta}sin\theta\right)j \tag{2.8}$$

The kinetic energy stored in the beam is:

$$T = \frac{1}{2}\int_0^l \rho A\left|\dot{R}\right|^2 dx = \frac{1}{2}\int_0^l \rho\left[(\dot{v} + x\dot{\theta})^2 + (v\dot{\theta})^2\right]dx \tag{2.9}$$

The strain (potential) energy stored in the beam is:

$$V = \frac{1}{2}\int_0^l EI(v'')^2\, dx \tag{2.10}$$

The kinetic and strain energies are substituted into the lagrangian defined as $L = T - V$ resulting:

$$L = \frac{1}{2}\int_0^l \left\{\rho A\left[\dot{v}^2 + 2\dot{v}x\dot{\theta} + (x\dot{\theta})^2 + (v\dot{\theta})^2\right] - EI(v'')^2\right\}dx \tag{2.11}$$

Substituting Equation (2.2) into Equation (2.11) – in other words, discretizing the lagrangian – results:

$$L = \frac{1}{2}\int_0^l \left\{\rho A\left[\left[\sum_{i=1}^n \emptyset_i(x)\dot{q}_i(t)\right]^2 + 2\left[\sum_{i=1}^n \emptyset_i(x)\dot{q}_i(t)\right]x\dot{\theta} + (x\dot{\theta})^2 + \left(\left[\sum_{i=1}^n \emptyset_i(x)q_i(t)\right]\dot{\theta}\right)^2\right] - EI\left(\left[\sum_{i=1}^n \emptyset''_i(x)q_i(t)\right]\right)^2\right\}dx \tag{2.12}$$

Substituting L into the Lagrange's equation given by:

$$\frac{d}{dt}\left[\frac{\partial L}{\partial \dot{q}_i}\right] - \frac{\partial L}{\partial q_i} = Q_i \tag{2.13}$$

and eliminating the terms whose derivatives are equal to zero results:

$$\frac{\rho A}{2}\frac{d}{dt}\left(\frac{1}{2}\left(\int_0^l \sum_{i=1}^{n}\sum_{j=1}^{n} \Phi_i\Phi_j\dot{q}_i\dot{q}_j\,dx\right)\right) + \rho A\frac{d}{dt}\left(\frac{\partial}{\partial\dot{q}_i}\left(\dot{\theta}\int_0^L x\sum_{i=1}^{n}\Phi_i\dot{q}_i dx\right)\right)$$

$$-\frac{\rho A}{2}\frac{\partial}{\partial q_i}\left(\dot{\theta}^2\int_0^l \sum_{i=1}^{n}\sum_{j=1}^{n} \Phi_i\Phi_j\dot{q}_i\dot{q}_j\,dx\right) + \frac{EI}{2}\frac{\partial}{\partial q_i}\left(\int_0^l \sum_{i=1}^{n}\sum_{j=1}^{n} \Phi_i^{"}\Phi_j^{"}\dot{q}_i\dot{q}_j\,dx\right)$$

$$= 0 \qquad (2.14)$$

Utilizing the identities:

$$\phi_i^{"}\phi_j^{"} = \phi_i^{iv}\phi_j \; and \; \phi^{iv} = \frac{\rho A\omega^2}{EI}\phi_i \qquad (2.15)$$

and applying the orthogonal principle:

$$\int_0^L \Phi_i\Phi_j dx = 1 \quad if \;\; i = j \; and \; \int_0^L \Phi_i\Phi_j dx = 0 \; i \neq j \qquad (2.16)$$

the following governing equation of motion is obtained:

$$\ddot{q}_i + \alpha_i\ddot{\theta} - \dot{\theta}^2 q_i + \omega_i{}^2 q_i = 0 \qquad (2.17)$$

where $\alpha_i = \int_0^L x\phi_i dx$.

In (FENILI, 2006), the extended Hamilton's principle is used to produce the same equations of motion (after proper discretization).

The following figures show the numerical solution of Equation (2.17) using the numerical integrator named forth order Runge-Kutta.

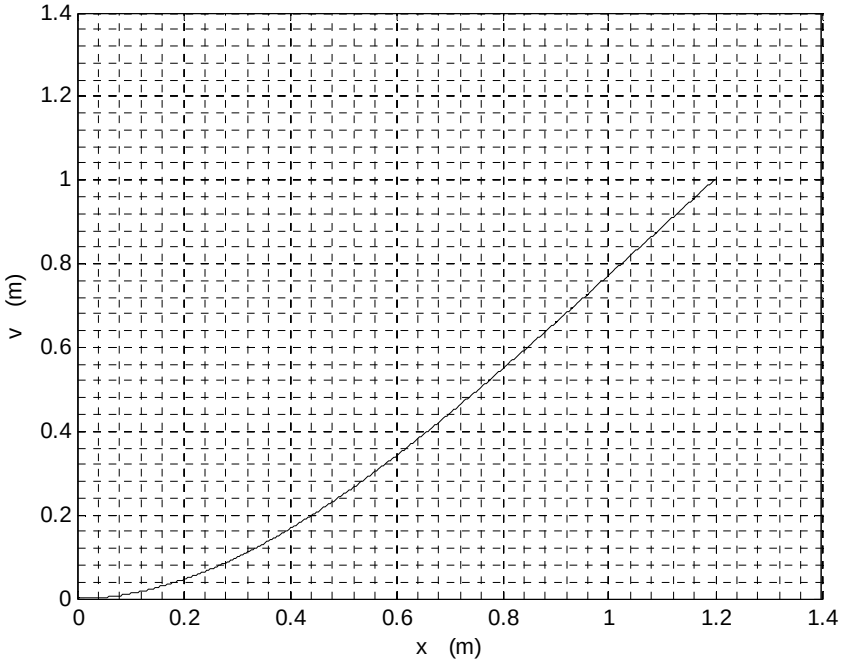

Fig 2.1 The first mode of vibration.

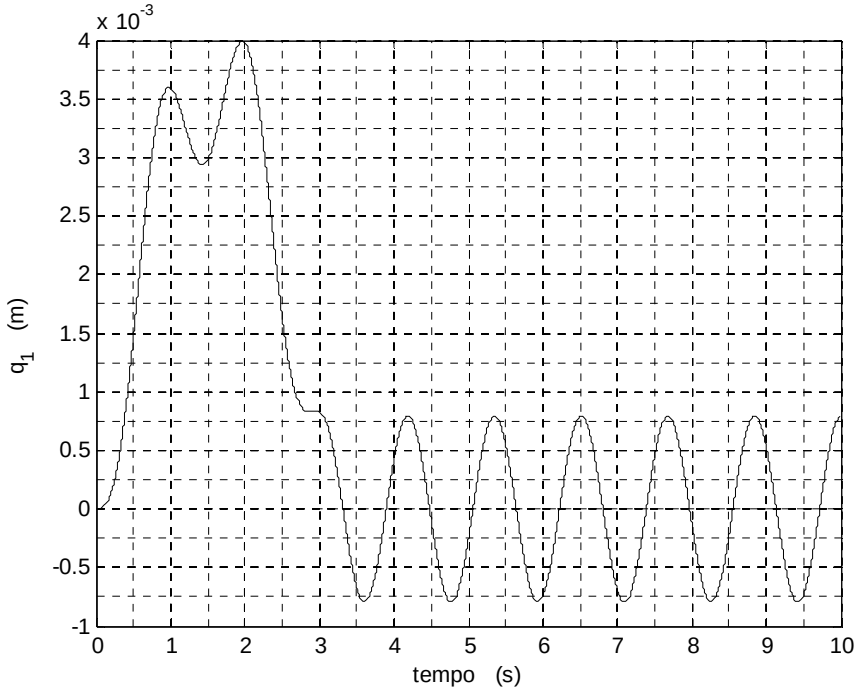

Figure 2.2 Tip displacement of the beam for the first mode of vibration.

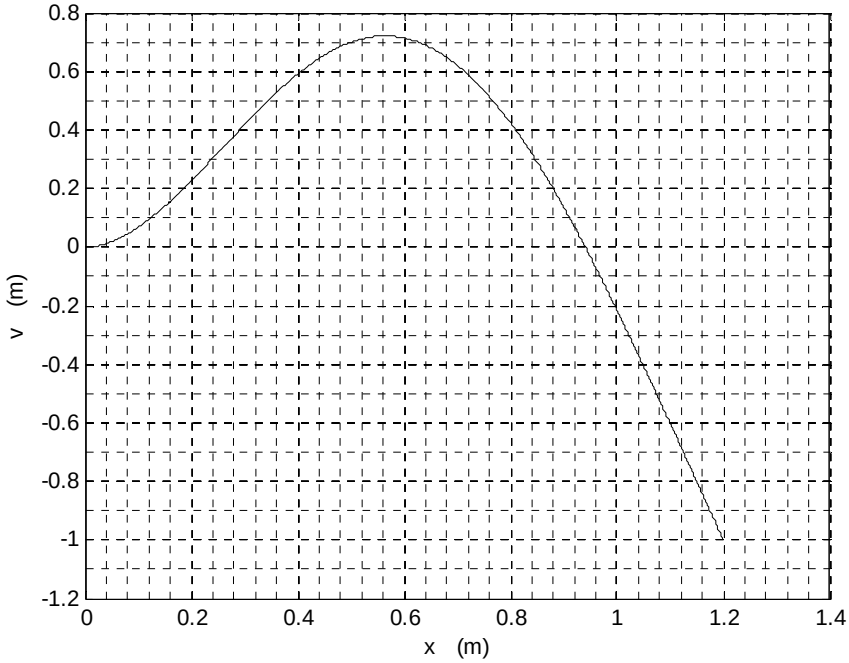

Fig 2.3 The second mode of vibration.

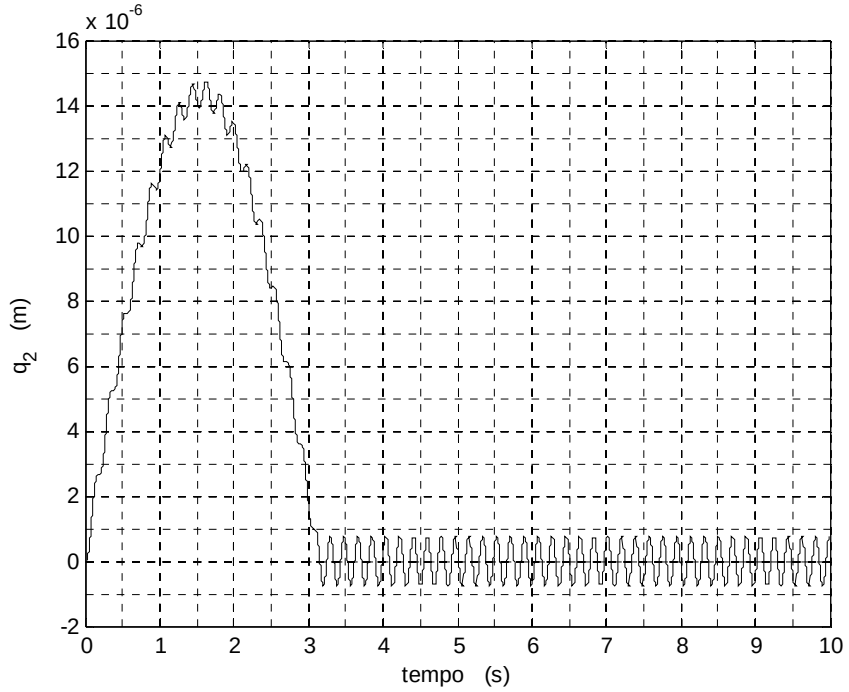

Figure 2.4 Tip displacement of the beam for the second mode of vibration.

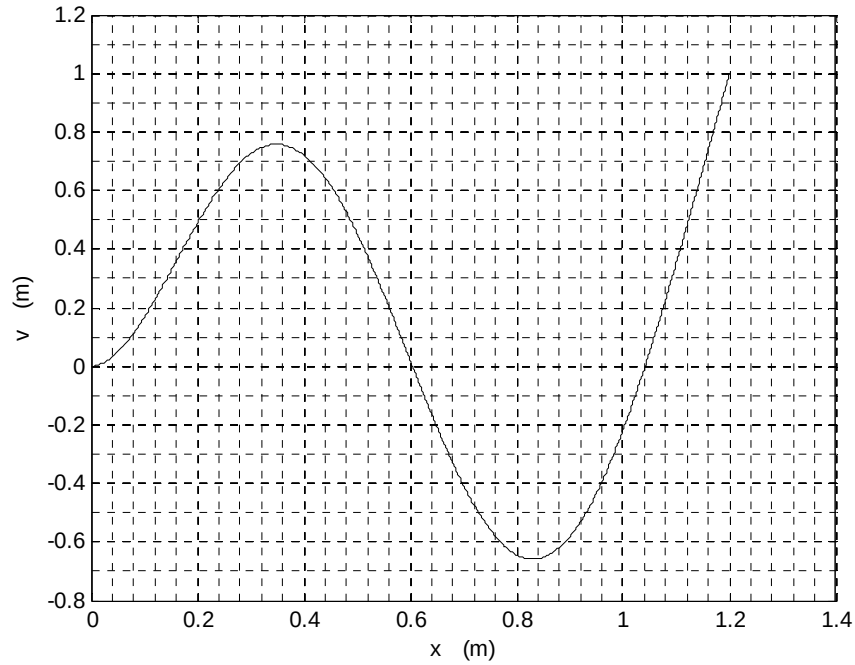

Fig 2.5 The third mode of vibration.

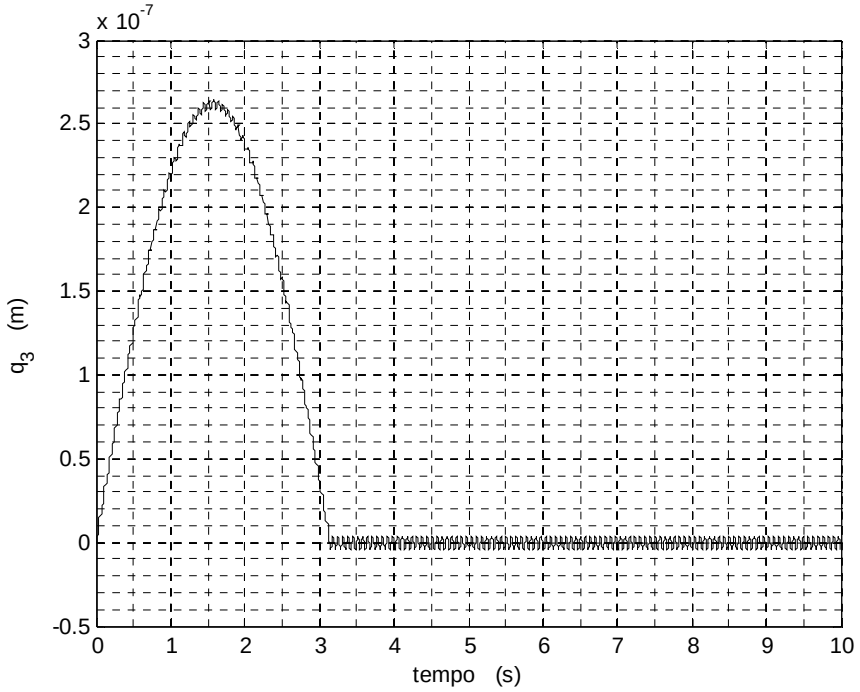

Figure 2.6 Tip displacement of the beam for the third mode of vibration.

CHAPTER 3

Including the Piezo in the Governing Equation of Motion

The use of piezoelectric ceramics to reduce vibration is a highly investigated topic in various applications. After having developed the equation of motion that describes the beam, the effects of the piezo need to be introduced.

3.1 The Piezoelectric actuator

There are some variations to the stating of the Piezo constitutive equations, depending of the direction of deformation and desired variables; however, here the following was obtained from (ZHANG, HE, & WANG, 2010) . The constitutive equations are used to obtain the voltage, or moment generated by the piezo. When used as a sensor, a known induced strain results in a dielectric displacement, which is solved for; and when employed as an actuator, the induced voltage would be given, and the stress solved for.

$$\{\sigma\} = -[c]\{E\} + [s]\{\varepsilon\} \tag{3.1}$$

$$\{D\} = [e]\{E\} + [c]\{\varepsilon\} \tag{3.2}$$

The following terms are the strain tensor matrix:$\boldsymbol{\varepsilon}$, the elastic stiffer constant matrix when the electric field $\boldsymbol{E}$is zero;$\boldsymbol{S}$, the stress tensor matrix;$\boldsymbol{\sigma}$, the piezoelectric stress constant;$\boldsymbol{c}$, the dielectric constant when the strain is zero;$\boldsymbol{e}$, and the electric displacement vector is given by $\boldsymbol{D}$.

The resulting equation of voltage obtained by (ZHANG, HE, & WANG, 2010) is given as:

$$V_i = ke_{31}b_p r_s \int_{x_{1i}}^{x_{2i}} \frac{\partial^2 w(x,t)}{\partial x^2} dx \tag{3.3}$$

The variables $i = 1, \dots, r, r\ and\ b_p$ are the number and width of the sensor respectively;r_s is the distance from the middle axis. In the given equation, voltage is amplified and multiplied by a constant k. This may be deemed as being similar if not equal to one divided by capacitance of the piezo.

Rearranging the variables the constitutive equation of the piezoelectric material can be given by:

$$\varepsilon_p = S_{pq}^E \sigma_q + d_{pi} E_i^e \tag{3.4}$$

where $\boldsymbol{S_{pq}}$ is the elastic compliance, $\boldsymbol{\sigma_p}$ is stress, $\boldsymbol{d_{pi}}$ is the piezoelectric strain constant, and $\boldsymbol{E_i^e}$ is the electric displacement. The subscript p indicates the stress direction on the perpendicular planes. If the piezoelectric layer is assumed to be free, the stress term σ_p would be zero, and the above equation reduced to:

$$\varepsilon_p = d_{31} \frac{V}{t_{ac}} \tag{3.5}$$

where V is the control voltage and t_{ac} is the thickness.

In (MOLTER, FONSECA, & BOTTEGA, 2009) the effect of the actuator is introduced as a moment given by:

$$M(x,t) = \int_{t_b/2}^{t_b/2+t_c} \sigma(x,t) b x dx = \int_{t_b/2}^{t_b/2+t_c} E_c \frac{d_{31} V(t)}{t_c} b x dx \tag{3.6}$$

An integral of the stress which is the young modulus of the piezo material (E_c) times the strain ($\varepsilon(x,t)$) induced by the piezo. The final moment is expressed as:

$$M(x,t) = \frac{1}{2} E_c d_{31} b (t_b + t_c) V(t) \tag{3.7}$$

In (DADFARNIA, JALILI, LIU, & DAWSON, 2004) the authors investigate the minimization of vibration on a robotic arm, which was modelled as a beam, and attached to a base with a translational motion. The layer of piezo is accounted for in the following manner: a coordinate system is defined where the x-axis is defined along the length, and the z-axis is defined along the height. The neutral axis of the beam along the cross section of the height is

considered to be zero($z = 0$). The section of the beam fitted with the piezo as an actuator has a neutral axis Z_n given by:

$$Z_n = \frac{c_{11}^p t_p (t_p + t_p)}{c_{11}^b t_b + c_{11}^p t_p} \tag{3.8}$$

The area affect by the induced strain ε is given by:

$$\varepsilon = \begin{cases} -z\frac{\partial^2 w(x,t)}{\partial x^2}, & for\ x < l_2\ \ or\ x > l_2 \\ -(z - z_n)\frac{\partial^2 w(x,t)}{\partial x^2}, & for\ l_1 < x < l_{2,} \end{cases} \tag{3.9}$$

Figure 3.1 presents some constants used in this work.

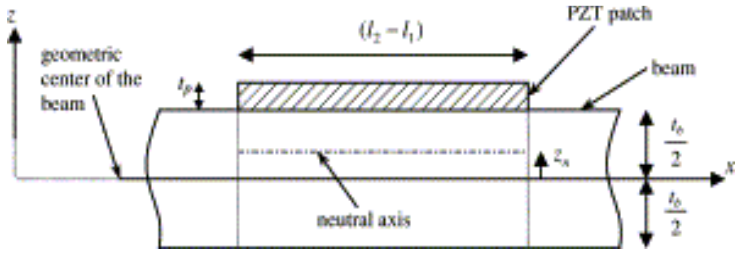

Figure 3.1 Configuration used by (DADFARNIA, JALILI, LIU, & DAWSON, 2004)

3.2 The derivation of the piezo force and strain equations

The following is the development of the piezo force and strain terms as done by (YOUSEFI-KOMA, 1997). First, the strain induced by the piezo effect is a result of an induced voltage $v$provided by the sensor. The following equation is used for a rectangular piezo actuator with positive polarization.

$$\wedge = \frac{d_{31a}}{t_a} v \tag{3.10}$$

where:

- t_a is the thickness
- d_{31a} is the strain constant

(YOUSEFI-KOMA, 1997) states that the stress-strain relationship of the piezoelectric material is laid out as being similar to that of thermoelastic materials and derived from (Kagawa and Gladwell 1970).

$$\sigma_a = E_a[\varepsilon_a - \wedge(x,y)] \tag{3.11}$$

where E_a,ε_a, and σ_a are the elastic modulus, strain, and stress of the piezo actuator.

The induced potential energy of the piezoelectric ceramic is given by:

$$u_a = \int_0^{\varepsilon_a} \sigma_a \, d\varepsilon_a \tag{3.12}$$

Making the substitution for the stress gives the resulting equation:

$$u_a = E_a \left[\frac{1}{2}\varepsilon_a^2 - \wedge(x,y)\varepsilon_a\right] \tag{3.13}$$

The total potential (strain) energy for the layer of piezo on the top and bottom is finally given by:

$$u_a = 2 \int_{(x_a - m_a)}^{(x_a + m_a)} \int_{t_b/2}^{-t_b/2} \int_{W_{a1}}^{W_{a2}} E_a \left[\frac{1}{2}\varepsilon_a^2 - \wedge(x,y)\varepsilon_a\right] d_y d_z d_x \tag{3.14}$$

Here x_a and m_a are the midpoint position, and one half of the piezo actuator length in the X direction, $t_{b`1}$ is the beam thickness. $W_{a1}$and W_{a2} are the endpoint positions of the piezo actuators in the Y direction.

With the use of the shape function, $\Phi(x)$, the potential energy equation is written as:

$$u_a = 2 \int_{(x_a - m_a)}^{(x_a + m_a)} \int_{t_b/2}^{-t_b/2} E_a W_a \left[\frac{1}{2}\varepsilon_a^2 - \wedge_a(x,y)\varepsilon_a\right] d_z d_x \tag{3.15}$$

The induced strain caused by the piezo electric effect gives as:

$$\Lambda_a = \frac{d31a}{t_a}\psi \tag{3.16}$$

Assuming that the piezo is perfectly bonded to the beam, the piezo strain is given in terms of:

$$\varepsilon_a = sgn(z)\left(\frac{2}{t_b}\right)\varepsilon_{tb}^{s} z; \quad \frac{t_b}{2} \leq |z| < \frac{t_b}{2} + t_a \tag{3.17}$$

where ε_{tb}^{s} is the total surface strain generated from the piezo and other external forces:

$$\varepsilon_{tb}^{ts} = -\frac{t_b}{2}\frac{\partial^2 v}{\partial x^2} \tag{3.18}$$

The finally derived equation for the potential energy of the piezo actuator:

$$U_a = \frac{1}{2}\left(\frac{1}{2}E_a W_a t_a t_b^2\right)\left(\frac{4}{3}t^{-2} + 2\bar{t} + 1\right)\int_{(x_a - m_a)}^{(x_a + m_a)} \frac{\partial^2 v}{\partial x^2} dx + (E_a W_a d_{31a} t_b)(\bar{t} + 1)\int_{(x_a - m_a)}^{(x_a + m_a)} \Psi \frac{\partial^2 v}{\partial x^2} V d_x \tag{3.19}$$

where:

$$\bar{t} = \frac{t_a}{t_b} \tag{3.20}$$

The modal expansion of the potential energy gives:

$$U_a = \frac{1}{2}\sum_{i=1}^{\infty}\sum_{j=1}^{\infty} q_i q_j k_{ij}^{piezo} - \sum_{i=1}^{\infty} Q_i^{piezo} q_i \tag{3.21}$$

In Equation (3.21), the stiffness matrix of the piezo actuator is given by:

$$K_{ij}^{piezo} = \frac{1}{2}(E_a W_a t_a t_b^2)(\frac{4}{3}\bar{t}^2 + 2\bar{t} + 1)\int_{(x_a - m_a)}^{(x_a + m_a)} \left(\frac{d^2\phi_i}{dx^2}\right)\left(\frac{d^2\phi_j}{dx^2}\right) dx \tag{3.22}$$

and the modal force of the piezo actuator is given by:

$$Q_i^{piezo} = -(E_a w_a d_{31a} t_b)(\bar{t} + 1)\int_{(x_{a-m_a})}^{(x_a + m_a)} \psi \frac{d^2\phi_i}{dx^2} dx \tag{3.23}$$

For a rectangular shaped piezo the parameter ψ is equivalent to 1, and only one piezo actuator and the sensor are going to be used.

Several pairs of piezo actuators would result in:

$$k_{ij}^{t} = \sum_{l=1}^{na} k_{ij}^{piezo,1} \tag{3.24}$$

$$Q_i^t = \sum_{l=1}^{na} Q_1^{piezo,1} \tag{3.25}$$

Finally the modal force and piezo stiffness are added to the equation of motion of the flexible beam through the Lagrangian of the whole system and the governing equations are derived again. In the final equation is included a term that accounts for the structural damping.

$$\ddot{q}_\iota + \alpha_i \ddot{\theta} + \left(k + \omega_i^2 - \dot{\theta}^2\right) q_i = Q_1 \tag{3.26}$$

Including in Equation (3.26) a term that accounts for the structural damping the governing equation results finally:

$$\ddot{q}_\iota + \alpha_i \ddot{\theta} + \left(k + \omega_i^2 - \dot{\theta}^2\right) q_i + \mu \dot{q_1} = Q_1 \tag{3.27}$$

The term in the right side of Equation (3.26) is expanded and better developed in the following. This term can be rewritten as:

$$\ddot{q}_\iota + \alpha_i \ddot{\theta} + \left(k + \omega_i^2 - \dot{\theta}^2\right) q_i + \mu \dot{q_1} = C \int_{x_1}^{x_2} \frac{d^2 \emptyset}{dx^2} \tag{3.28}$$

or:

$$\ddot{q}_\iota + \alpha_i \ddot{\theta} + \left(k + \omega_i^2 - \dot{\theta}^2\right) q_i + \mu \dot{q_1} = C \int_{x_1}^{x_2} \frac{d}{dx}\left(\frac{d\emptyset}{dx}\right) dx \tag{3.29}$$

or:

$$\ddot{q}_\iota + \alpha_i \ddot{\theta} + \left(k + \omega_i^2 - \dot{\theta}^2\right) q_i + \mu \dot{q_1} = C \int_{x_1}^{x_2} \frac{d}{dx} \phi' \tag{3.30}$$

or:

$$\ddot{q}_\iota + \alpha_i \ddot{\theta} + \left(k + \omega_i^2 - \dot{\theta}^2\right) q_i + \mu \dot{q_1} = C\left(\phi'(x_2) - \phi'(x_1)\right) \tag{3.31}$$

The parameter C in Equation (3.31) is $C = -(E_a w_a d_{31a} t_b)(\bar{t} + 1)$.

3.3 The Heaviside Function

Here one presents an alternative way to obtain the expression on the right side of Equation (3.31).

Using the extended Hamilton´s principle one obtains the partial differential governing equation for an undamped clamped free Euler-Bernoulli beam with external moment from the piezo as given by:

$$EIv^{iv} + \rho A\ddot{v} = M \tag{3.32}$$

or:

$$EI\frac{\partial^4 v}{\partial x^4} + \rho A\frac{\partial^2 v}{\partial t^2} = M \tag{3.33}$$

Applying the assumed modes method in Equation (3.33):

$$EI\sum \phi_i{}^{iv} q_i + \rho A\sum_{i=1}^{m} \phi_i \ddot{q}_\iota = M \tag{3.34}$$

or:

$$\sum_{i=1}^{m}[EI\phi_i{}^{iv} q_i + \rho A\phi_i \ddot{q}_\iota] = M \tag{3.35}$$

Multiplying the governing equation by the mode ϕ_i results:

$$\phi_j \sum_{i=1}^{m}[EI\phi_i{}^{iv} q_i + \rho A\phi_i \ddot{q}_\iota] = \phi_j M \tag{3.36}$$

Applying now the orthogonal rule given by Equation (2.16) and the identity given by Equation (2.17) and integrating from 0 to *l* results:

$$\phi_j \sum_{i=1}^{m}[EIq_i \int_0^l \phi_i^{iv}\phi_j dx + \rho A\phi_i \ddot{q}_\iota \int_0^l \phi_i\phi_j\, dx] = \int_0^l M\phi_j \tag{3.37}$$

or:

$$\sum_{i=1}^{m}[EIq_i\, \omega^2 \int \phi_i\phi_j dt + \rho A\ddot{q}_i] = \int_0^l M\phi_j \tag{3.38}$$

The Heaviside function is employed in the form:

$$H(x) = H(x - x_{a1}) - H\big(x - (x_{a1} + l_{a1})\big) \tag{3.39}$$

where x_{a1} and l_{a1} represent the position and length of the piezo material. After substitution in to the right side of the governing equation of motion:

$$\sum_{i=1}^{m}[EIq_i\,\omega^2 \int \phi_i\phi_j dt + \rho A\ddot{q}_i] = Q_{ax}\int_0^{L_b}\frac{\partial^2 H}{\partial x^2}\emptyset_1\,dx \tag{3.40}$$

or, finally:

$$\sum_{i=1}^{m}[EIq_i\,\omega^2 \int \phi_i\phi_j dt + \rho A\ddot{q}_i] = Q(-1)^1[\emptyset'(x_{a1}) - \emptyset'(x_{a1} + l_{a1})] \tag{3.41}$$

The final version of the governing equation is teh same as presented before:

$$\ddot{q}_i + \alpha_i\ddot{\theta} + \big(k + \omega_i^2 - \dot{\theta}^2\big)q_i + \mu\dot{q_1} = Q(-1)^1[\emptyset'(x_{a1}) - \emptyset'(x_{a1} + l_{a1})] \tag{3.42}$$

CHAPTER 4

The PD and LQR Linear Controllers

4.1 THE PD controller

The Proportional and derivative control actions as stated by (Harijonon, Jafari, Wiriadidjaja, & Ahmad, 2015), the proportional feedback constant is responsible for the natural frequency of the system and the amplitude of vibration, with the integral constant being able to affect the system damping. Working jointly, steady state error is reduced while simultaneously diminishing the effect of system disturbances. It was observed in the model developed that it required large gain values from the proportional gain to affect the system; hence, the use of the proportional gain might be better when always paired with an integral. The use of large gain values however, still produce reasonable voltages, in positions of the piezo where the system tended towards stability; however, using large gain values would require more robust, larger, and hence, more expensive amplifies.

The proportion and derivative are applied to the voltage signal generated by the sensor and sent to the actuator in a closed loop relationship:

$$V_a = -K_p V_s - K_d \frac{\partial V_s}{\partial t} \tag{4.1}$$

In (SHUEEI-MUH, 2007), the effects of the variation of k_d and k_p on the vibration frequency are expressed graphically, when $k_d = 0$. It is stated that the decrease of the proportional gain causes an increase in the oscillation frequency and irrespective of proportional gain, varying derivative gain from zero cause the frequency of oscillation to decrease. More importantly, it is stated that neglecting the derivative gain will not result in active damping of a rotating beam.

4.2 The LQR (Linear Quadratic Regulator)

The Liner Quadratic Regulator is referred to as an optimal control. The main idea is to develop a control law u(t) that minimizes the a cost function:

$$J_{LQR} := \int_0^{\infty} z(t)' Qz(t) + \rho u'(t) Ru(t) dt \tag{4.2}$$

where $z(t)$ the states matrix, $u(t)$ the input matrix, Q is a symmetric positively defined $\ell \, x \, \ell$ matrix , and R is also symmetric and positively defined $m \, x \, m$ matrix. The aim of the LQR is to minimize the values of the both the inputs and states.

Both matrices $Q$and R are selected by trial and error, these positively weighted matrices allow from optimization of control gains, and by adjusting values along the diagonals, different system variable can be weighted differently to achieve a required result, this can be shown by carrying of the multiplication of the states and weight matrices.

In order to apply the LQR control, the governing equation must be of the form:

$$\dot{x} = Ax + Bu \tag{4.3}$$

Hence the governing equation must be transformed to the state space from as shown:

$$\begin{Bmatrix} \dot{x_1} \\ \dot{x_2} \end{Bmatrix} = \begin{bmatrix} 0 & 1 \\ k - \omega^2 - \dot{\theta}^2 & -\mu \end{bmatrix} \begin{Bmatrix} x_1 \\ x_2 \end{Bmatrix} + \begin{bmatrix} 0 & 0 \\ 0 & -\alpha \end{bmatrix} \begin{Bmatrix} 0 \\ \ddot{\theta} \end{Bmatrix} + \begin{bmatrix} 0 & 0 \\ 1 & 0 \end{bmatrix} \begin{Bmatrix} Q \\ 0 \end{Bmatrix} \tag{4.4}$$

For the numerical simulations one considers:

$$A = \begin{bmatrix} 0 & 1 \\ k - \omega^2 & -\mu \end{bmatrix} \tag{4.5}$$

$$B = \begin{bmatrix} 0 & 0 \\ Q & 0 \end{bmatrix} \tag{4.6}$$

Nonlinearities are neglected in order to find the LQR gains. The A matrix is also modified according to Equation (4.5), neglecting the time dependent term. The gains obtained, however, are used in the complete governing equation, with all the neglected terms.

CHAPTER 5

Numerical Results

Table 5.1 presents a general overview for each position of the piezo in each mode, interchanging with the LQR and PD controllers. In some position, the vibration was being amplified instead of diminished; those positions were defined as being unstable.

	1st mode	2nd mode	3rd mode
Root	PD Fig 5.1	PD Fig 5.7	PD Fig 5.13(US)
	LQR Fig 5.19	LQR Fig 5.25	LQR Fig 5.31
Center	PD Fig 5.3	PD Fig 5.9 (US)	PD Fig 5.15
	LQR Fig 5.21	LQR Fig 5.27	LQR Fig 5.33
End	PD Fig 5.5	PD Fig 5.11 (US)	PD Fig 5.17
	LQR Fig 5.23	LQR Fig 5.29	LQR Fig 5.35

Table 5.1 Controllers and positions of the piezo for each mode. US = unstable.

The results of the PD and LQR controls will be demonstrated on the modes of vibration. The voltage value must be in the range of $120V > V_{max} > -120V$, which is the stated break down voltage for the PZT piezo material.

5.1 First mode of vibration: PD with K_p = 22000 and K_d =6000

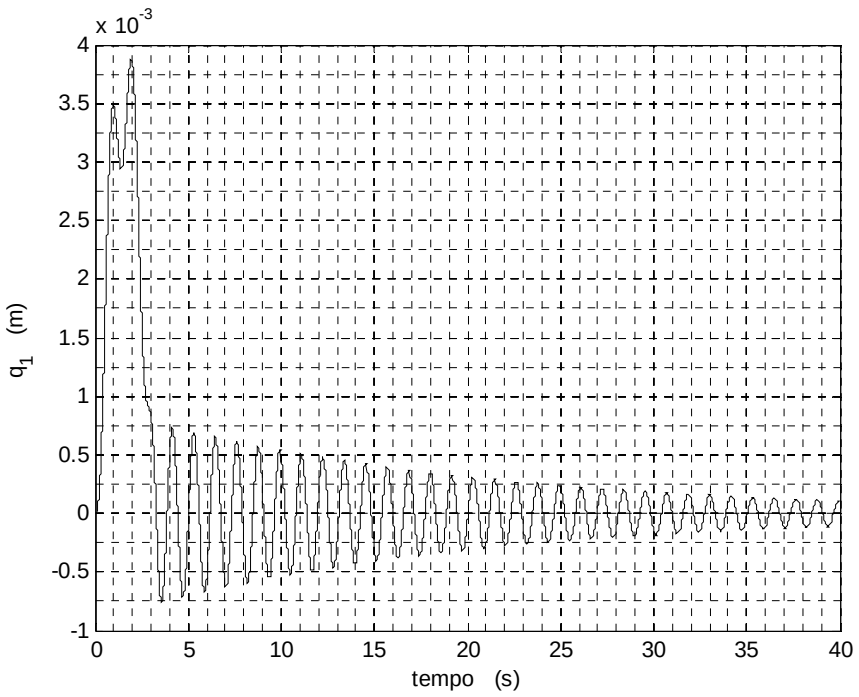

Figure 5.1 Tip displacement. Piezo at the root of the beam. First mode.

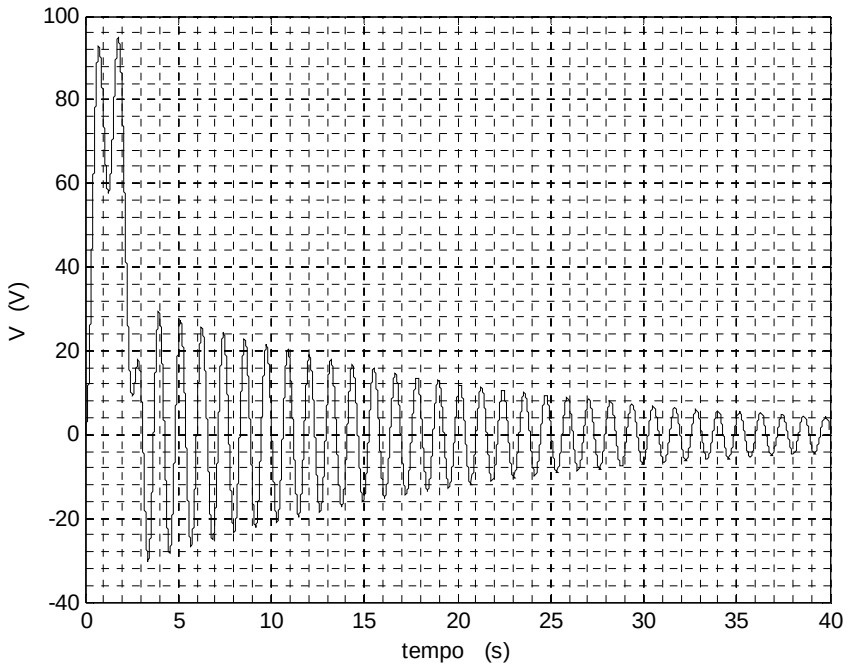

Figure 5.2 Voltage signal for the first mode of vibration (piezo at the root of the beam).

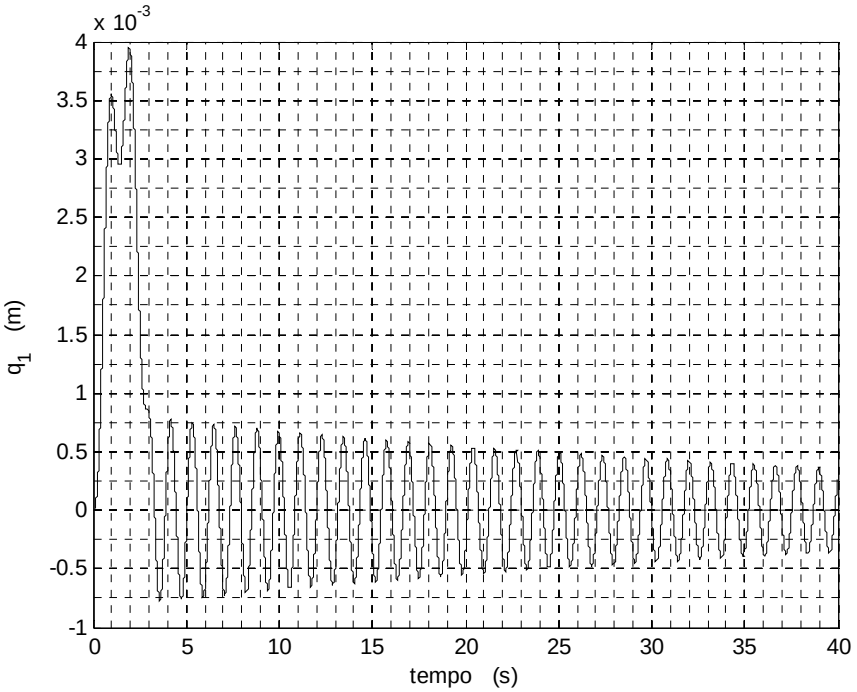

Figure 5.3 Tip displacement. Piezo at the center of the beam. First mode.

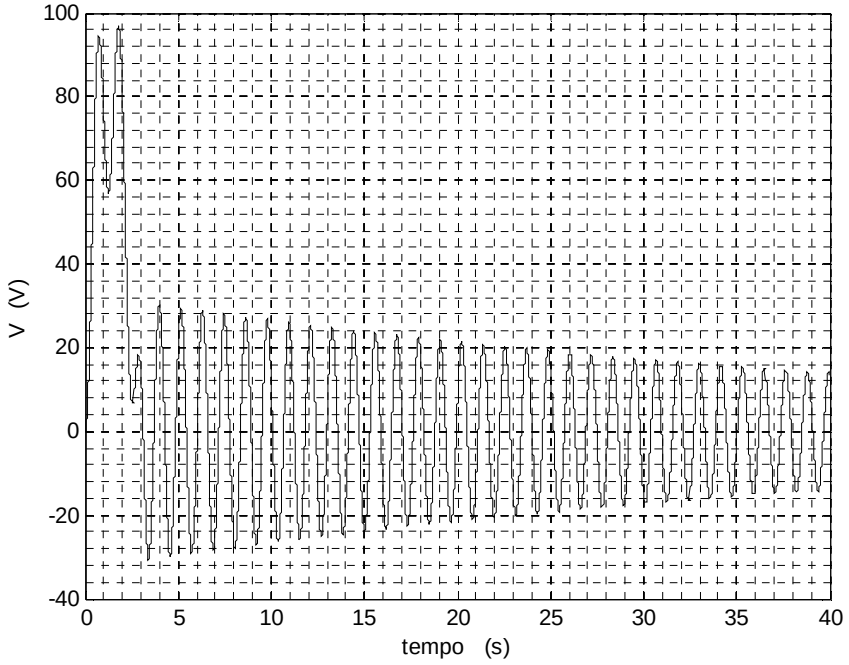

Figure 5.4 Voltage signal for the first mode of vibration (piezo at the center of the beam).

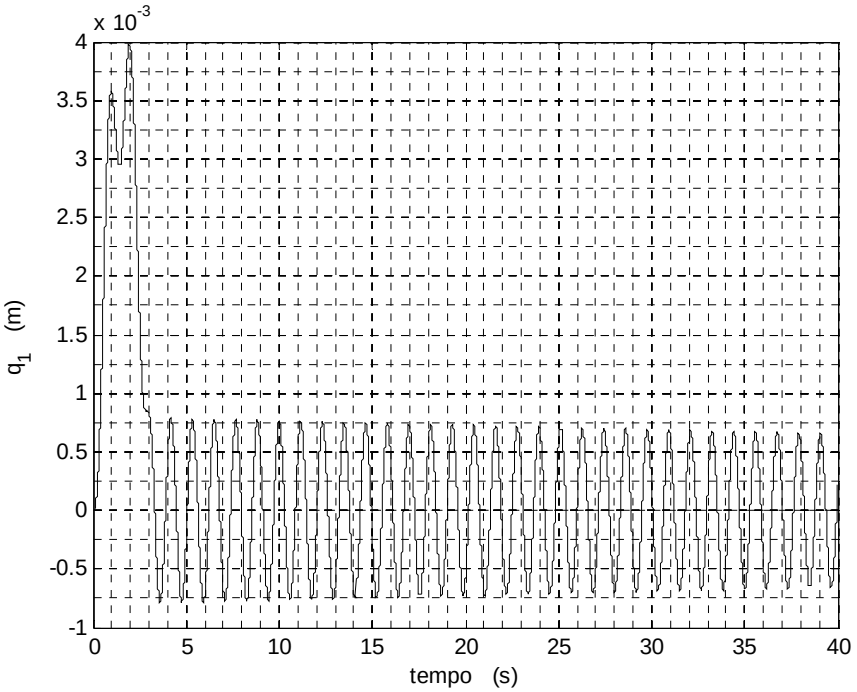

Figure 5.5 Tip displacement. Piezo at the end of the beam. First mode.

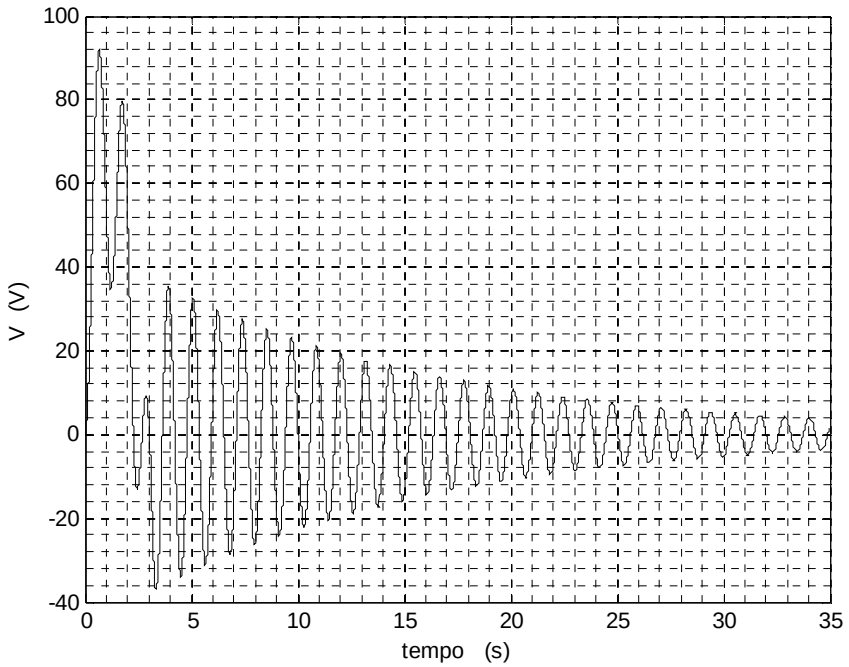

Figure 5.6 Voltage signal for the first mode of vibration (piezo at the end of the beam).

5.2 Second mode of vibration: PD

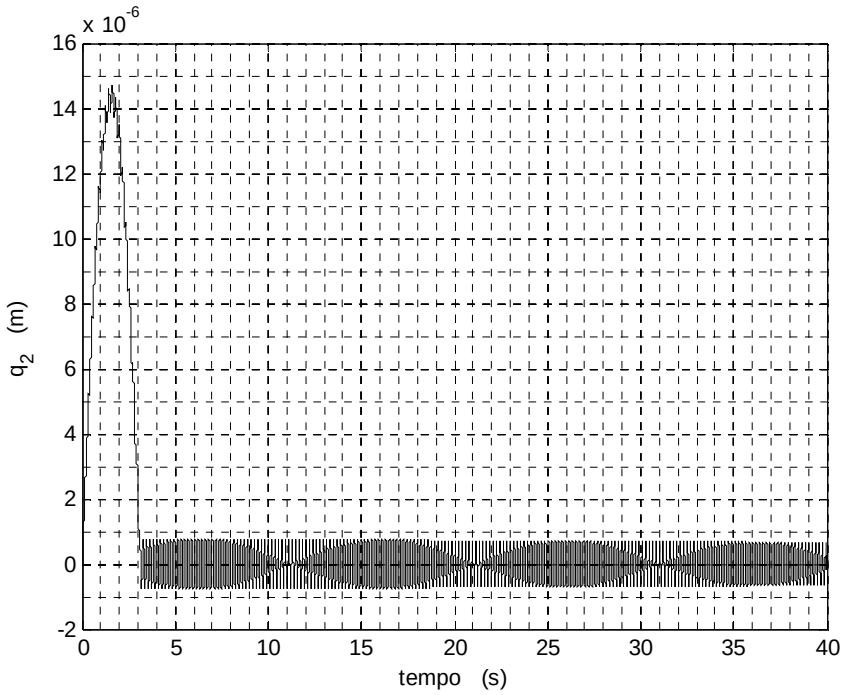

Figure 5.7 Tip displacement. Piezo at the root of the beam. Second mode. K_p = 1800000 and K_d =8000.

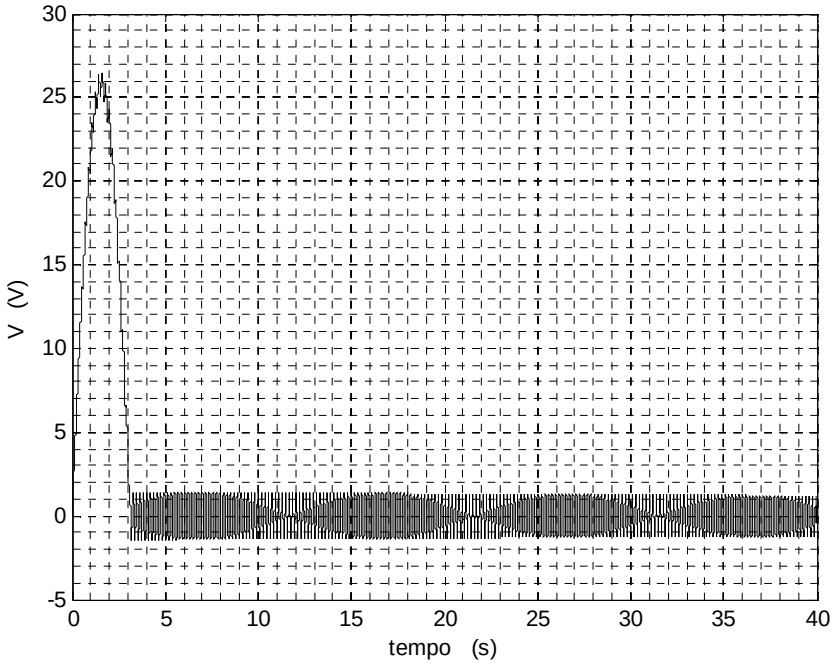

Figure 5.8 Voltage signal for the second mode of vibration (piezo at the root of the beam). K_p = 1800000 and K_d =8000.

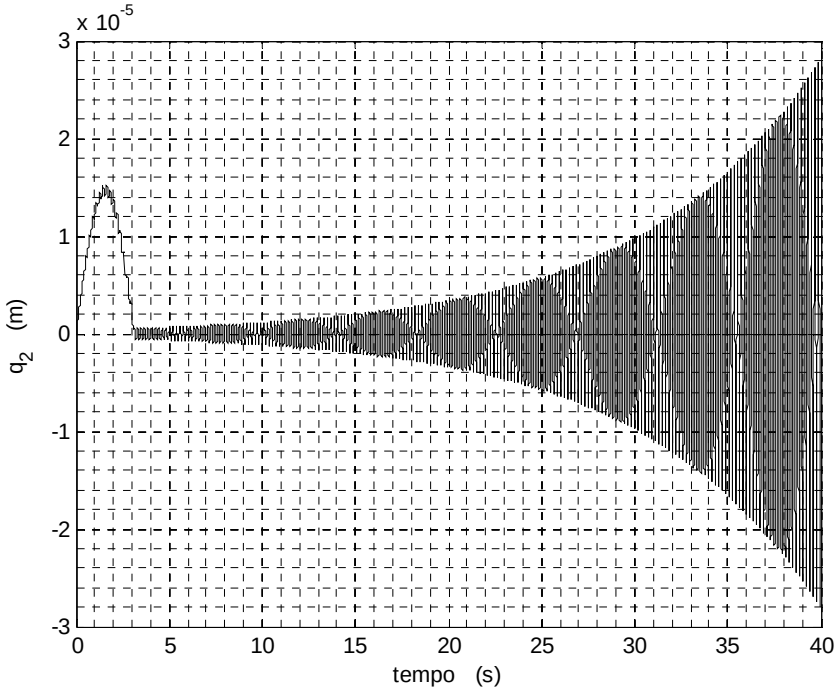

Figure 5.9 Tip displacement. Piezo at the center of the beam. Second mode. K_p = 100000 and K_d =1000.

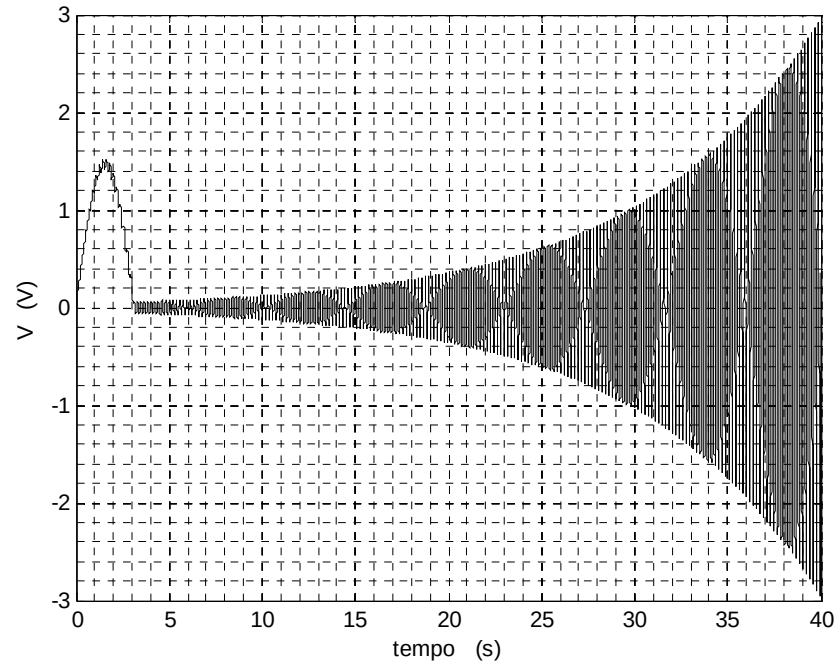

Figure 5.10 Voltage signal for the second mode of vibration (piezo at the center of the beam). K_p = 100000 and K_d =1000.

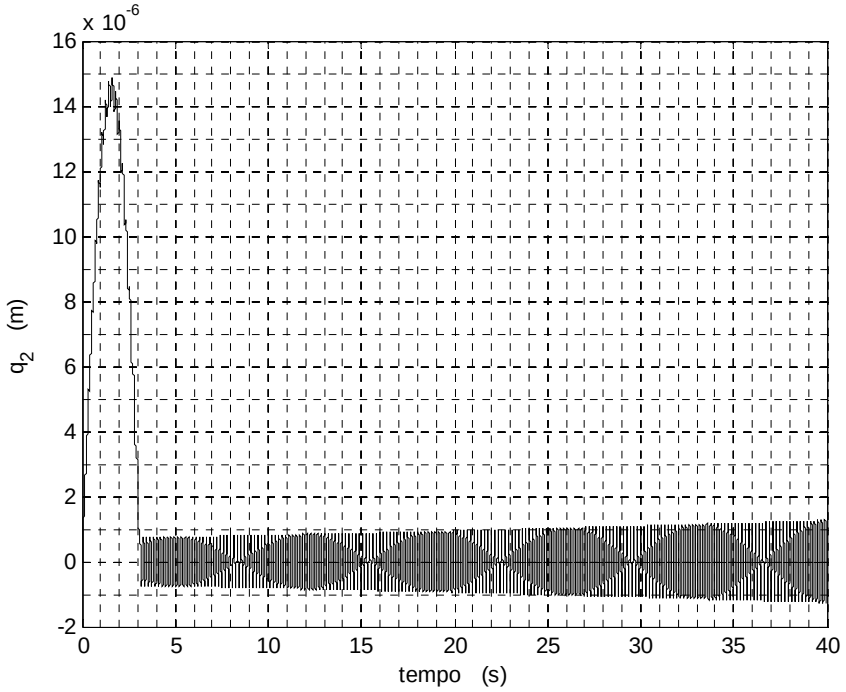

Figure 5.11 Tip displacement. Piezo at the end of the beam. Second mode. K_p = 1800000 and K_d =8000.

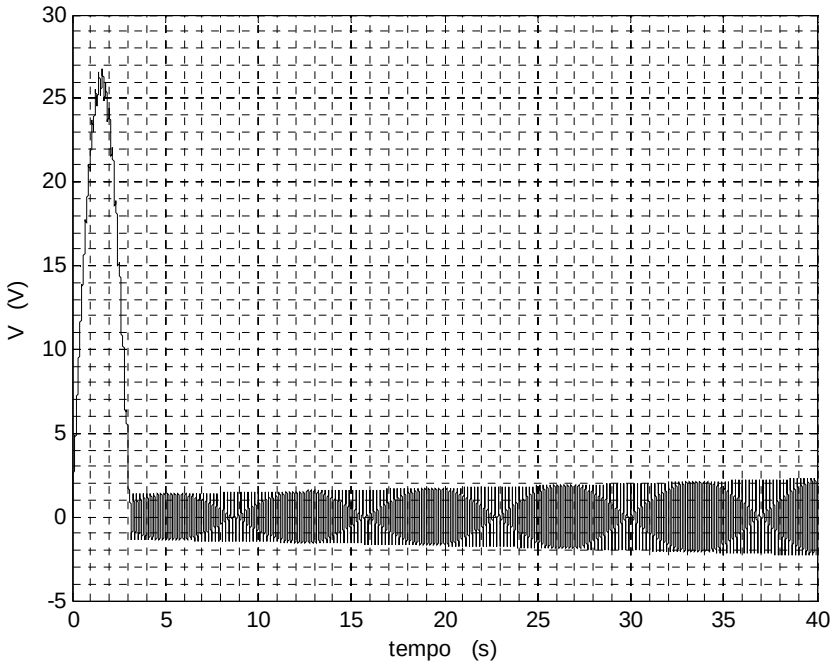

Figure 5.12 Voltage signal for the second mode of vibration (piezo at the end of the beam). K_p = 1800000 and K_d =8000.

5.3 Third mode of vibration: PD

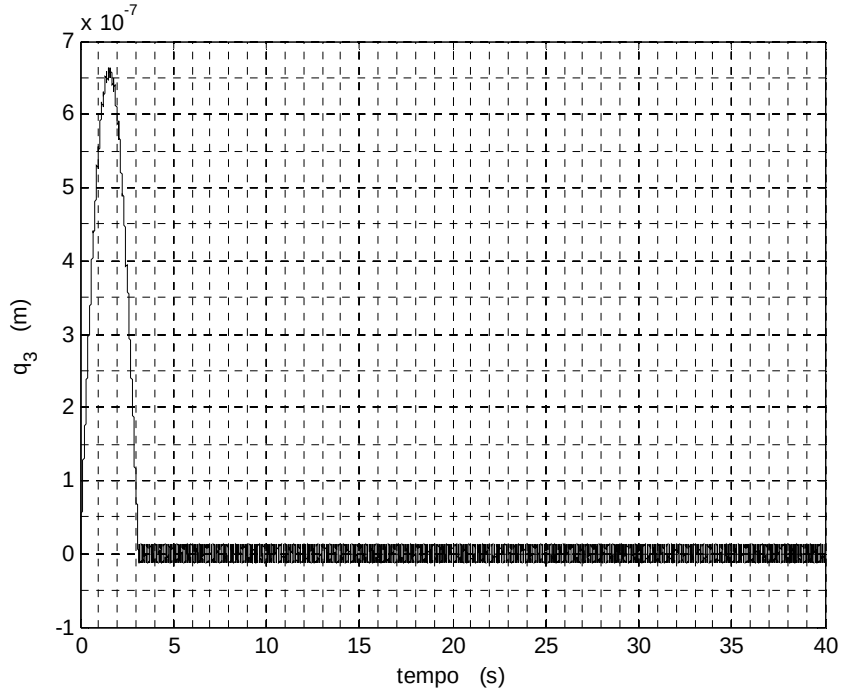

Figure 5.13 Tip displacement. Piezo at the root of the beam. Third mode. K_p = 0.18 and K_d =0.08.

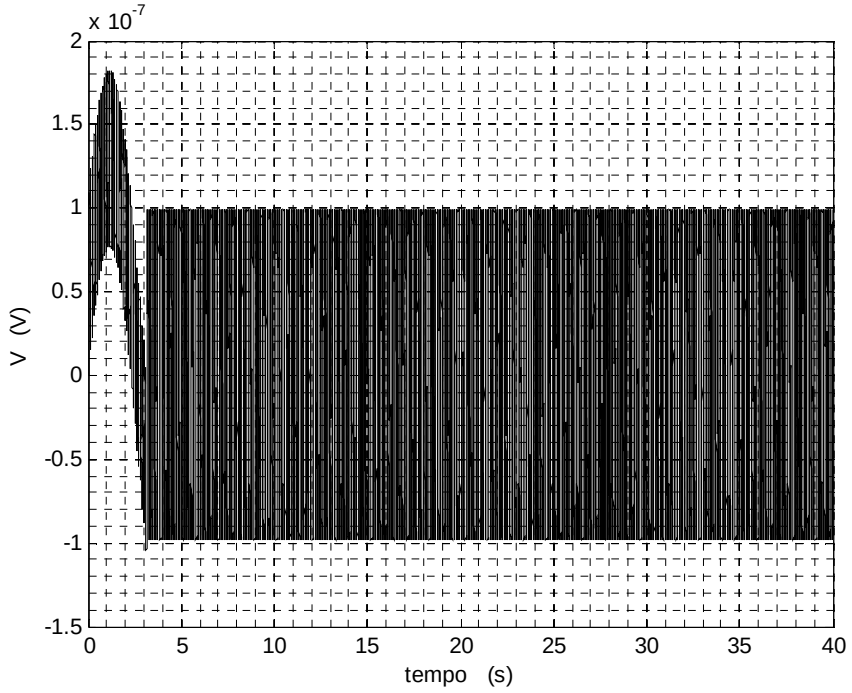

Figure 5.14 Voltage signal for the third mode of vibration (piezo at the root of the beam). K_p = 1800000 and K_d =8000.

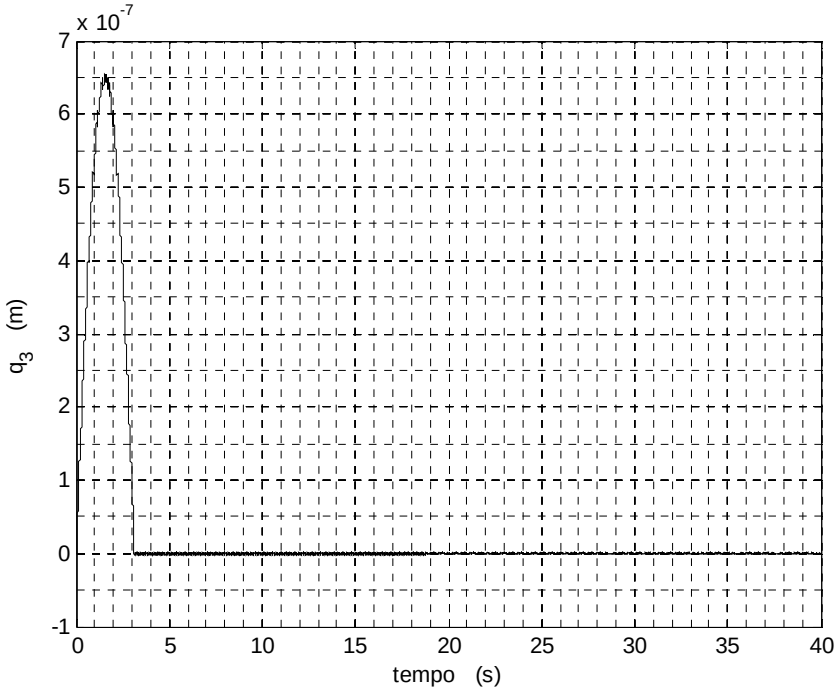

Figure 5.15 Tip displacement. Piezo at the center of the beam. Third mode. K_p = 7000000 and K_d =1000.

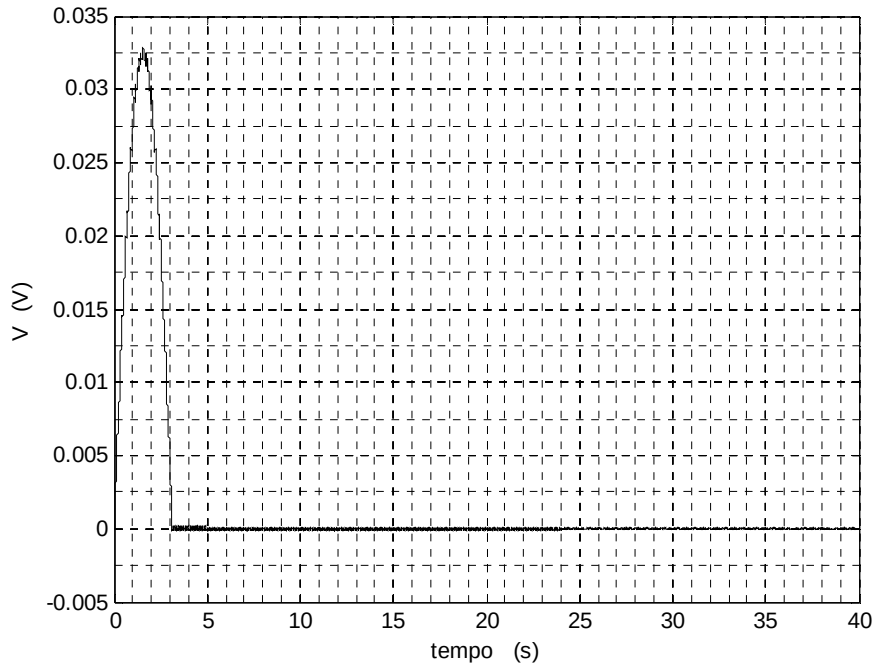

Figure 5.16 Voltage signal for the third mode of vibration (piezo at the center of the beam). K_p = 7000000 and K_d =1000.

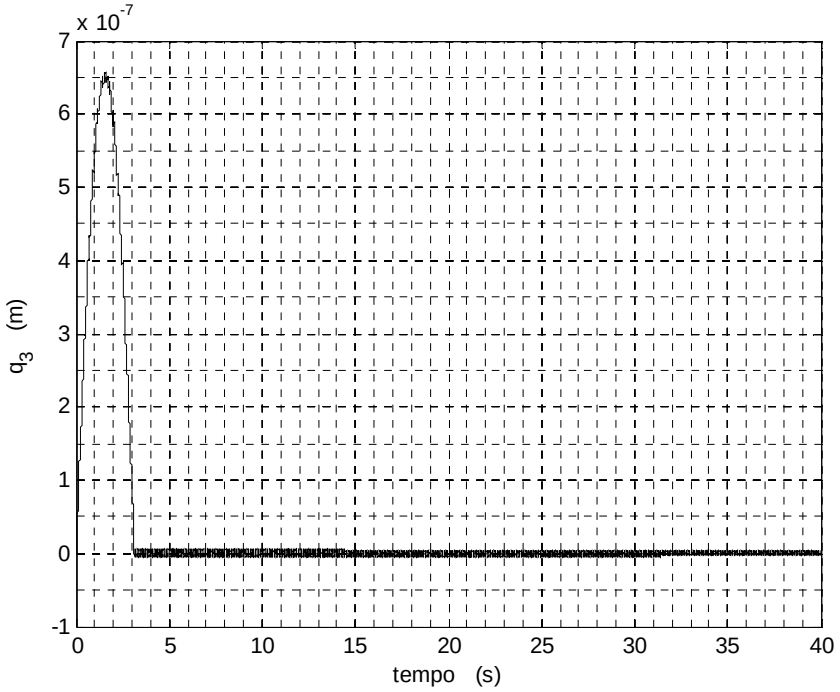

Figure 5.17 Tip displacement. Piezo at the end of the beam. Third mode. K_p = 55000 and K_d =300.

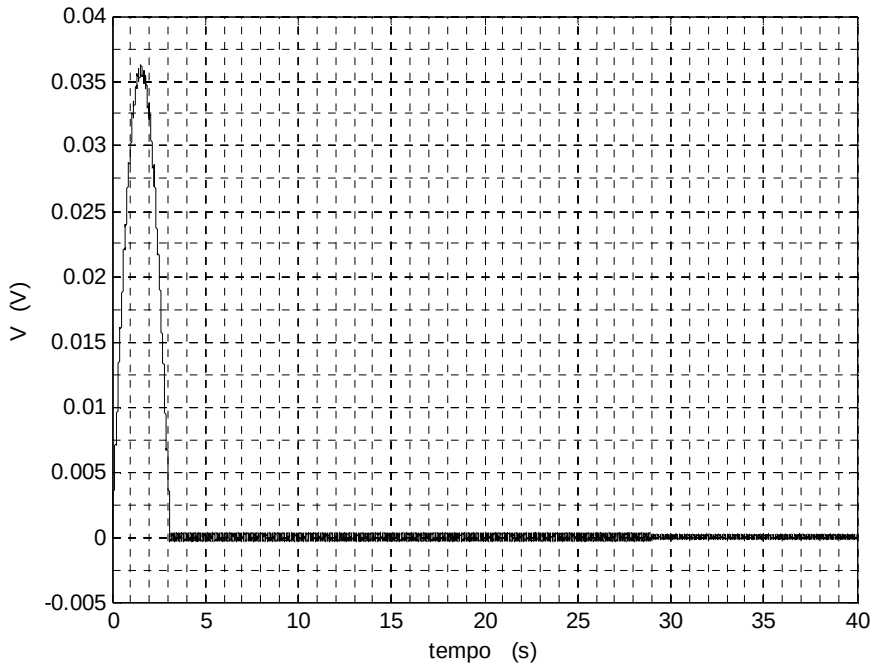

Figure 5.18 Voltage signal for the third mode of vibration (piezo at the end of the beam). K_p = 55000 and K_d =300.

5.4 First mode of vibration: LQR

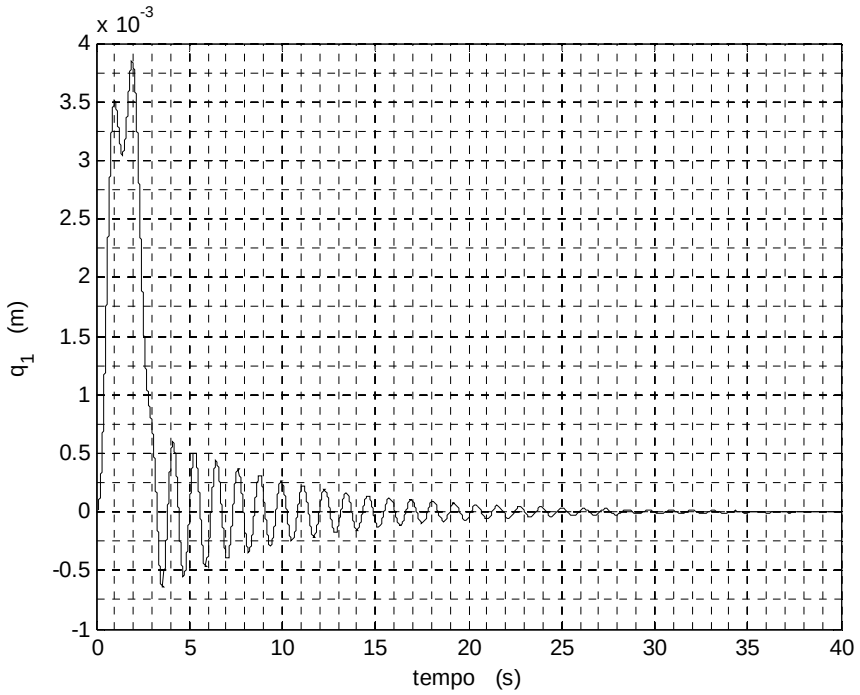

Figure 5.19 Tip displacement. Piezo at the root of the beam. First mode. R=[130 0 ; 0 1300] and Q=[30 0 ; 0 $3*10^{10}$].

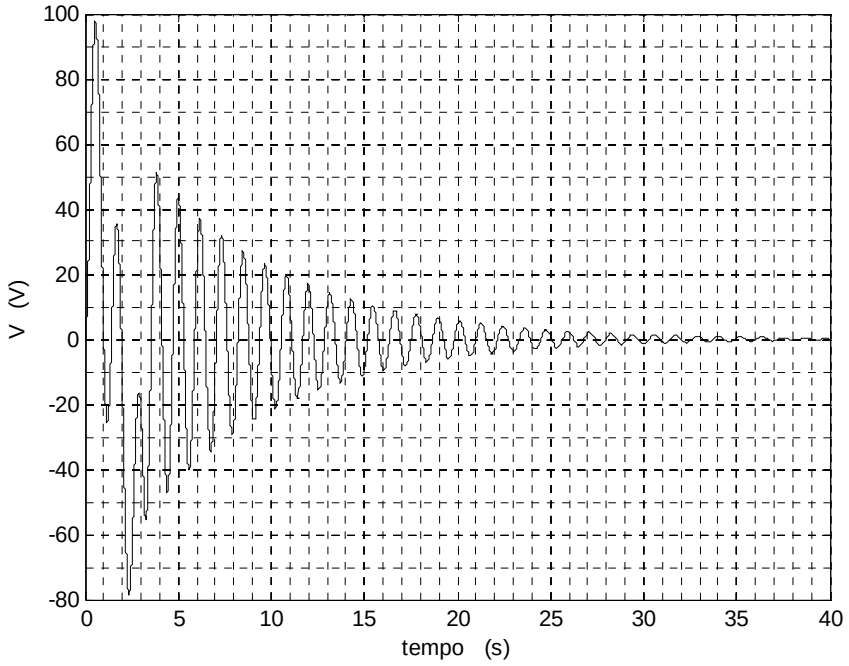

Figure 5.20 Voltage signal for the first mode of vibration (piezo at the root of the beam). R=[130 0 ; 0 1300] and Q=[30 0 ; 0 $3*10^{10}$].

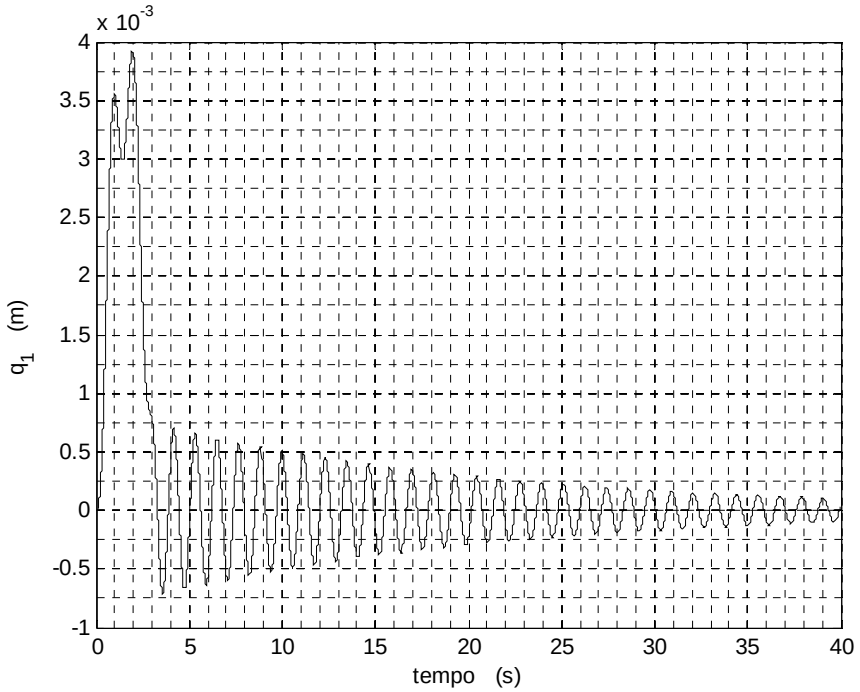

Figure 5.21 Tip displacement. Piezo at the center of the beam. First mode. R=[130 0 ; 0 1300] and Q=[30 0 ; 0 $3*10^{10}$].

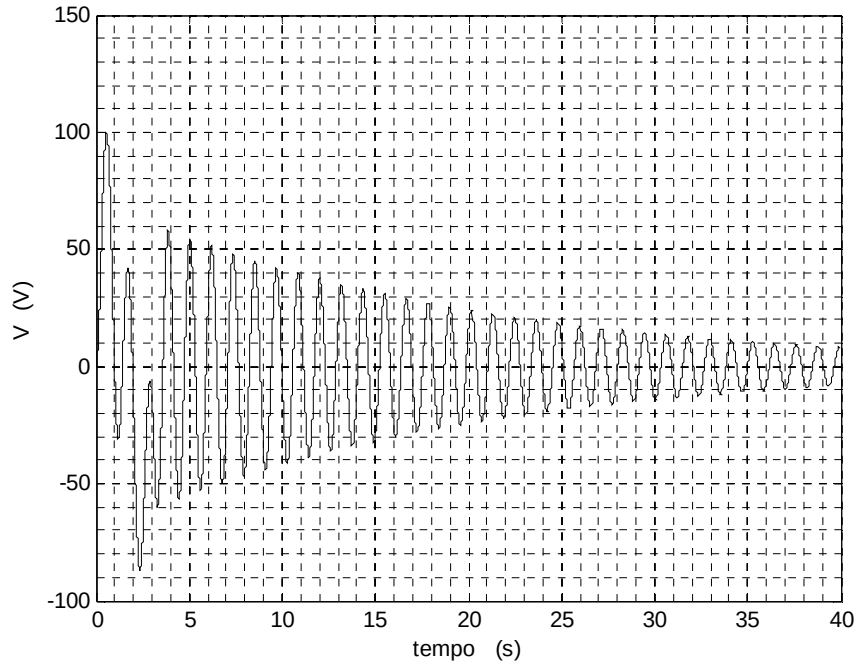

Figure 5.22 Voltage signal for the first mode of vibration (piezo at the center of the beam). R=[130 0 ; 0 1300] and Q=[30 0 ; 0 $3*10^{10}$].

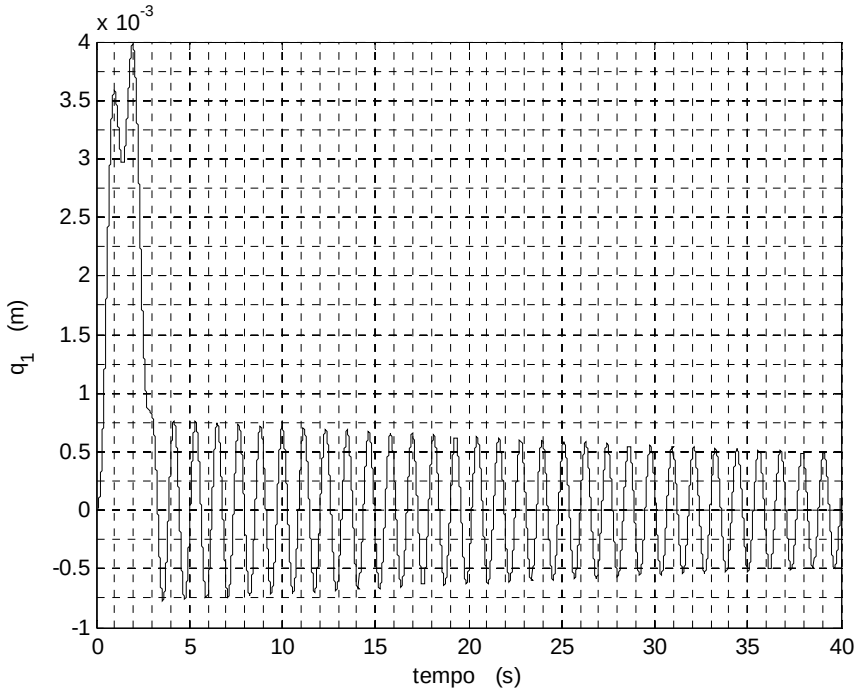

Figure 5.23 Tip displacement. Piezo at the end of the beam. First mode. R=[130 0 ; 0 1300] and Q=[30 0 ; 0 $3*10^{10}$].

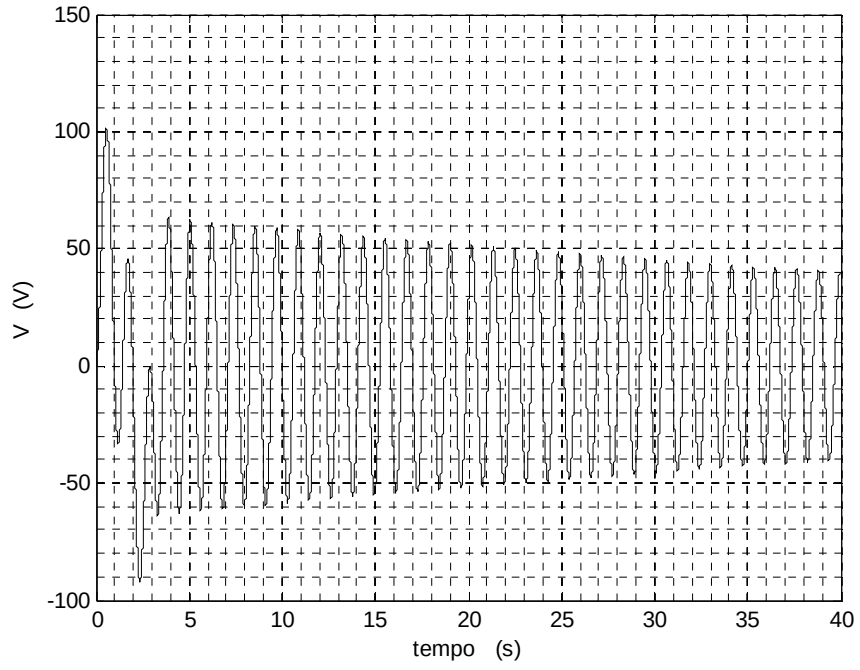

Figure 5.24 Voltage signal for the first mode of vibration (piezo at the end of the beam). R=[130 0 ; 0 1300] and Q=[30 0 ; 0 $3*10^{10}$].

5.5 Second mode of vibration: LQR

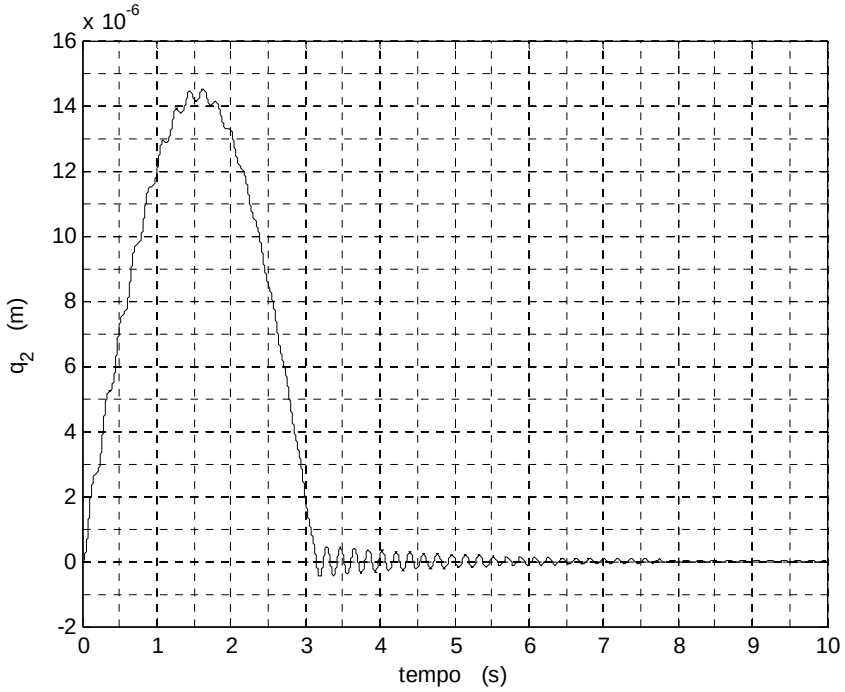

Figure 5.25 Tip displacement. Piezo at the root of the beam. Second mode. R=[0.13 0 ; 0 13] and Q=[10^6 0 ; 0 10^8].

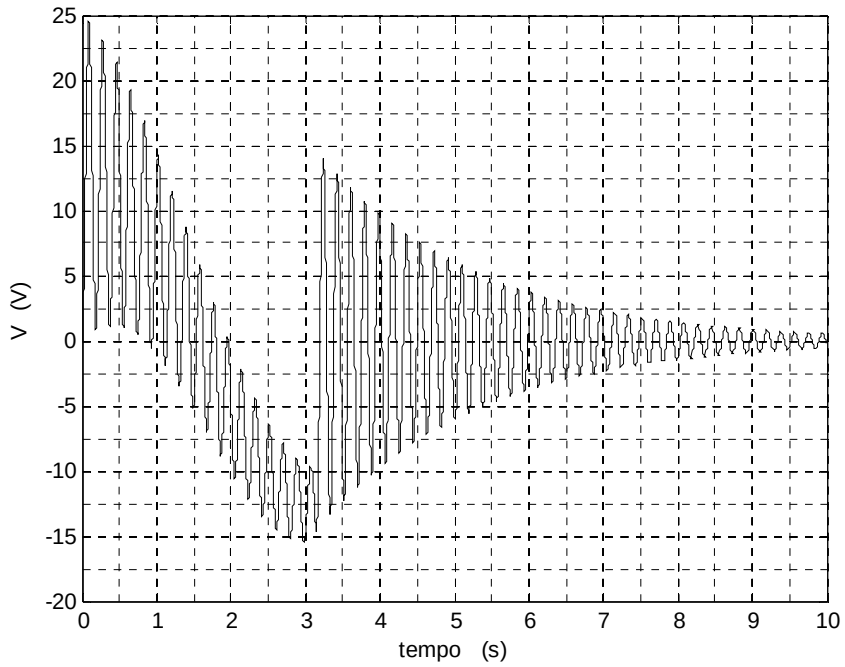

Figure 5.26 Voltage signal for the second mode of vibration (piezo at the root of the beam). R=[0.13 0 ; 0 13] and Q=[10^6 0 ; 0 10^8].

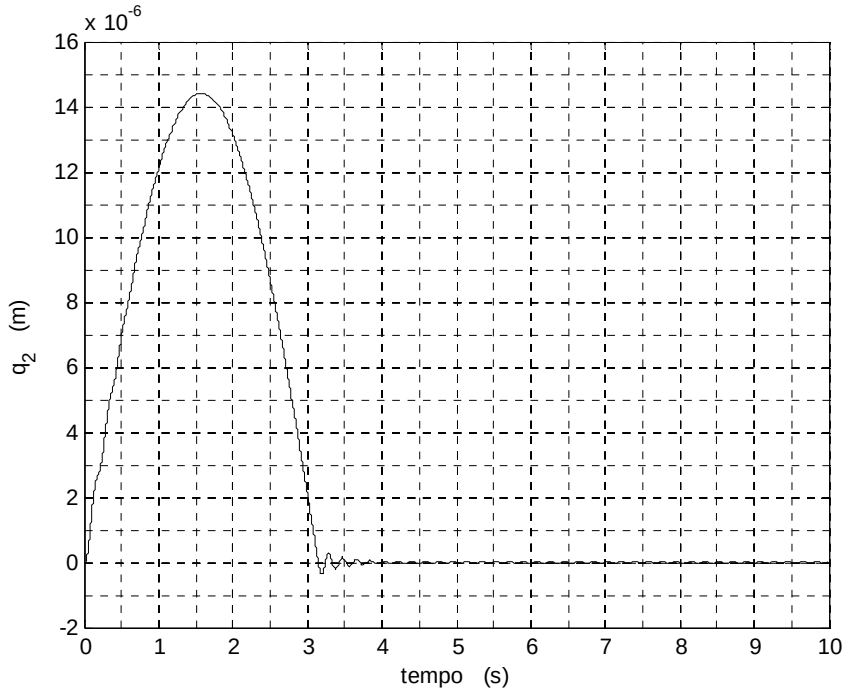

Figure 5.27 Tip displacement. Piezo at the center of the beam. Second mode. R=[0.13 0 ; 0 1.3] and Q=[10^4 0 ; 0 10^7].

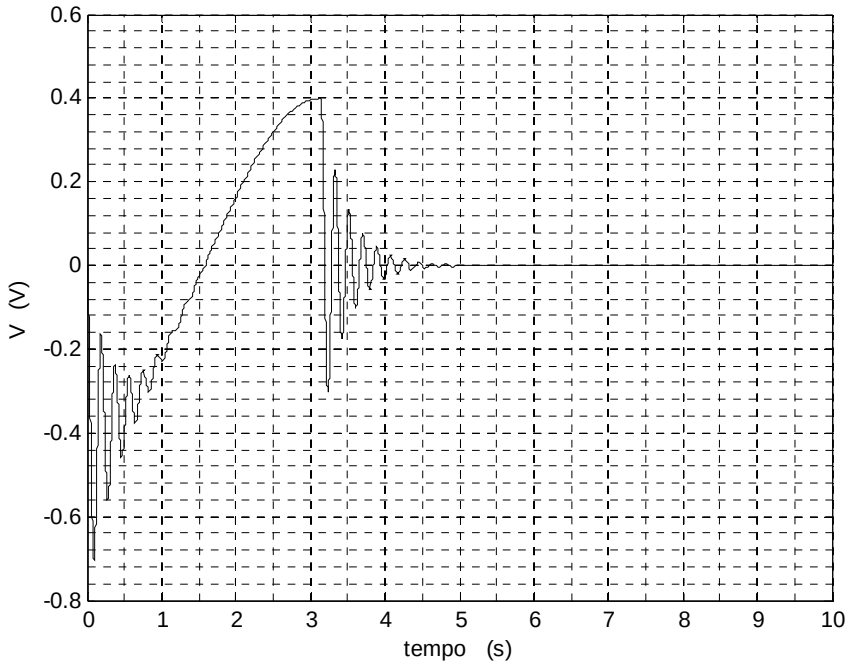

Figure 5.28 Voltage signal for the second mode of vibration (piezo at the center of the beam). R=[0.13 0 ; 0 1.3] and Q=[10^4 0 ; 0 10^7].

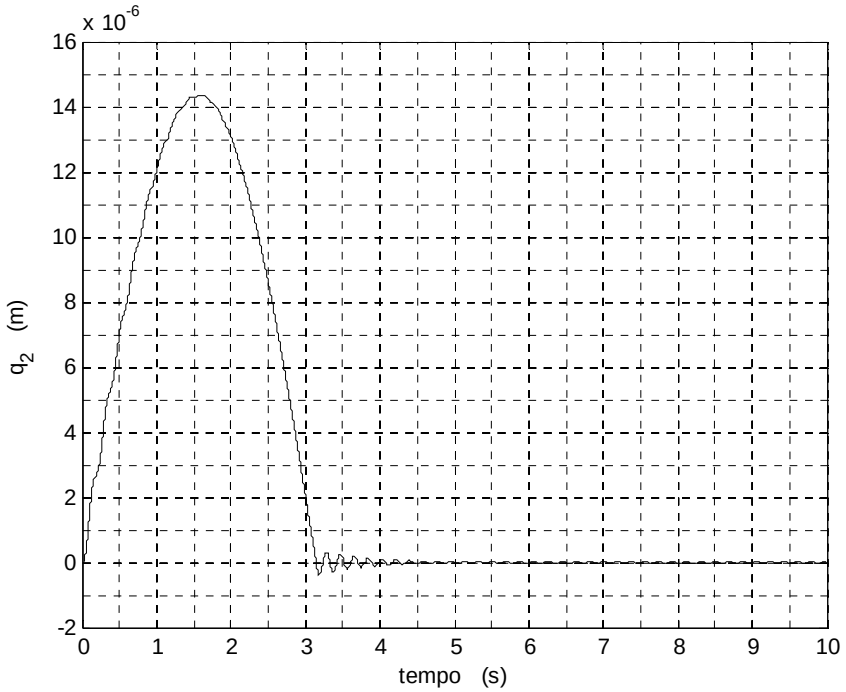

Figure 5.29 Tip displacement. Piezo at the end of the beam. Second mode. R=[0.13 0 ; 0 1.3] and Q=[10^6 0 ; 0 10^{10}].

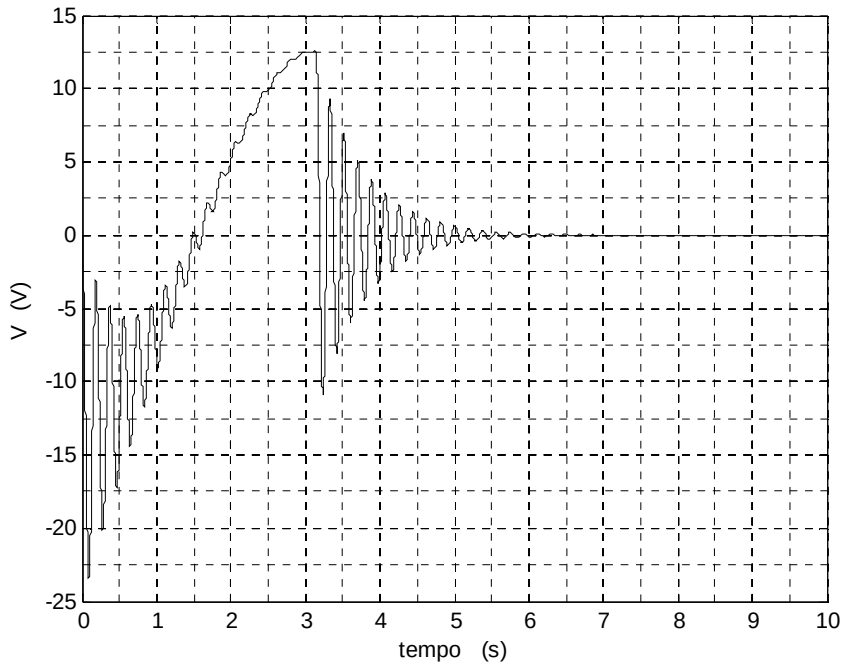

Figure 5.30 Voltage signal for the second mode of vibration (piezo at the center of the beam). R=[0.13 0 ; 0 1.3] and Q=[10^6 0 ; 0 10^{10}].

5.6 Third mode of vibration: LQR

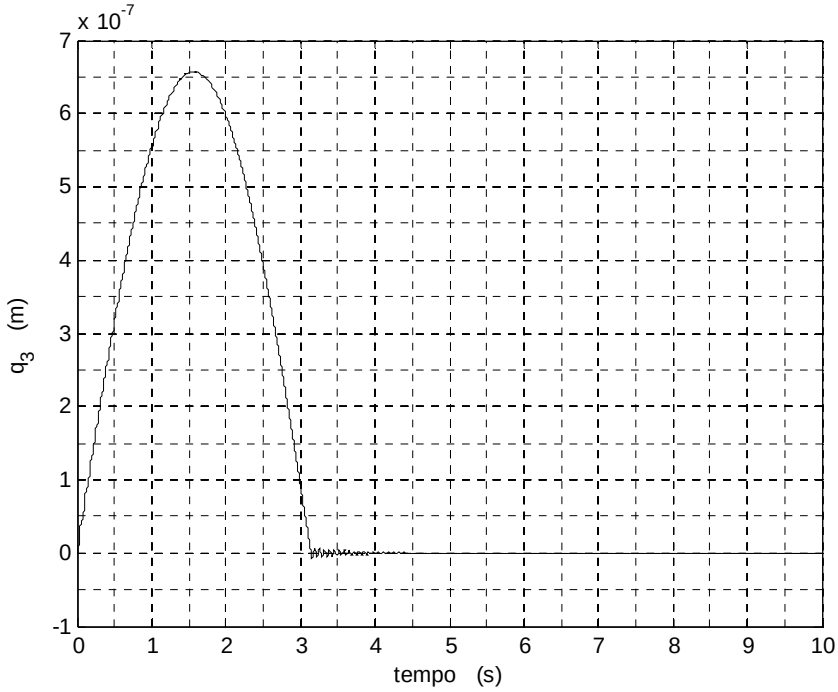

Figure 5.31 Tip displacement. Piezo at the root of the beam. Third mode. R=[0.13 0 ; 0 0.13] and Q=[10^8 0 ; 0 10^8].

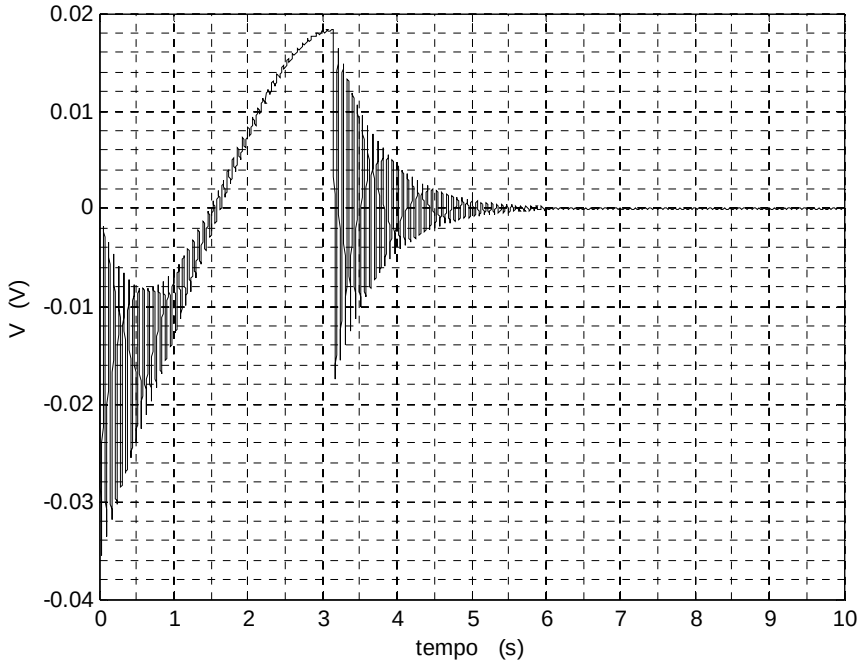

Figure 5.32 Voltage signal for the third mode of vibration (piezo at the root of the beam). R=[0.13 0 ; 0 0.13] and Q=[10^8 0 ; 0 10^8].

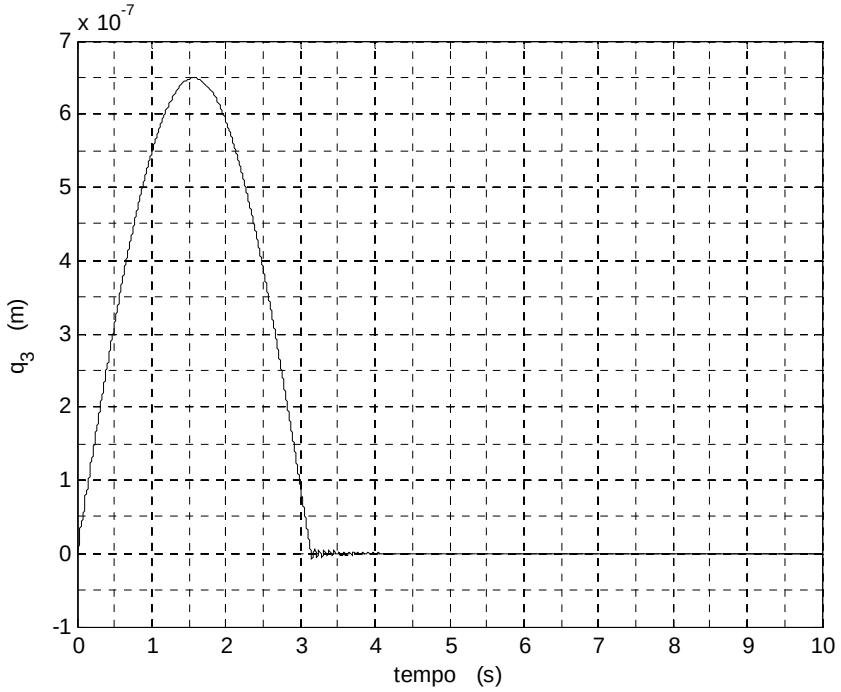

Figure 5.33 Tip displacement. Piezo at the center of the beam. Third mode. R=[0.13 0 ; 0 0.13] and Q=[10^5 0 ; 0 10^5].

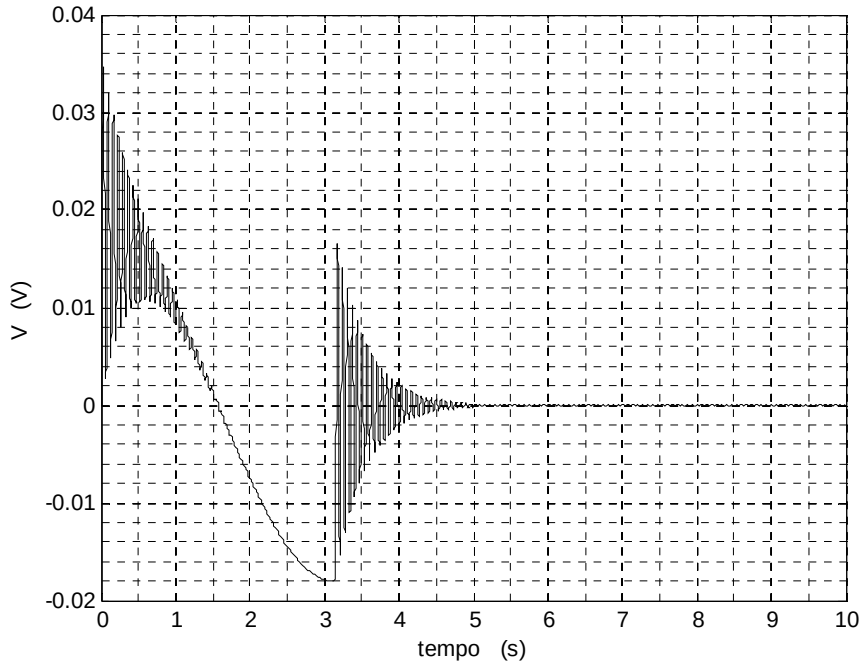

Figure 5.34 Voltage signal for the third mode of vibration (piezo at the center of the beam). R=[0.13 0 ; 0 0.13] and Q=[10^5 0 ; 0 10^5].

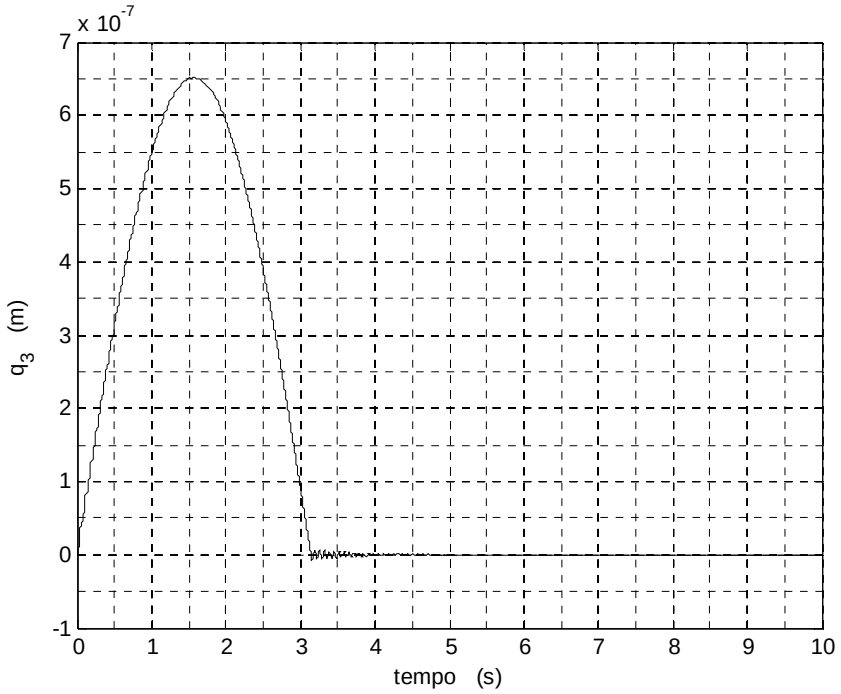

Figure 5.35 Tip displacement. Piezo at the end of the beam. Third mode. R=[0.13 0 ; 0 0.13] and Q=[10^6 0 ; 0 10^6].

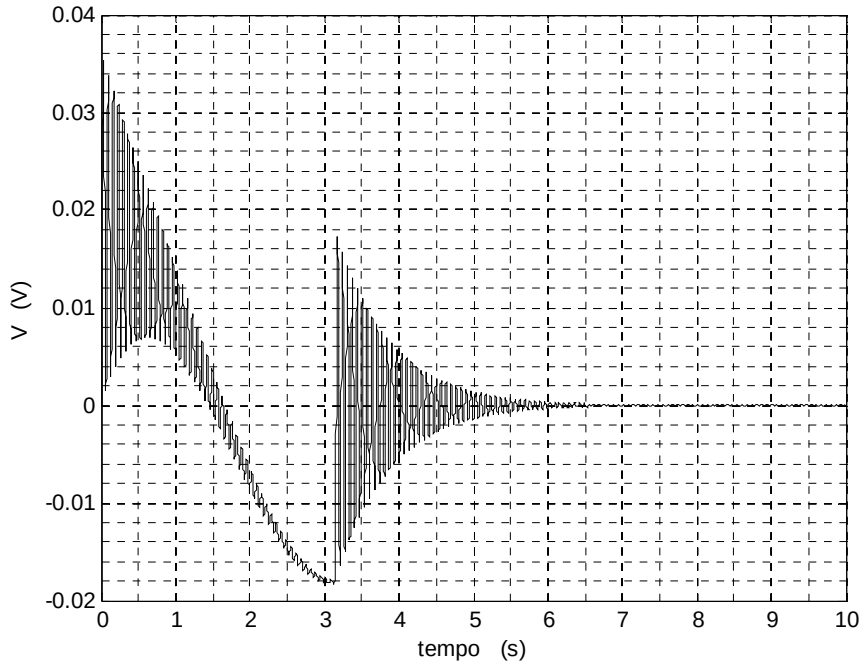

Figure 5.34 Voltage signal for the third mode of vibration (piezo at the ebd of the beam). R=[0.13 0 ; 0 0.13] and Q=[10^6 0 ; 0 10^6].

From the results presented, it can be seen that for the first and second modes, the most effective location of the piezo is at the root of the beam, while for the third mode, the center and end positions yielded results of vibration suppression.

For the second mode placement of the piezo in the center and end position leads toward amplification of the tip displacement; same applies to the place of the piezo in the first position (root) for the third mode of vibration.

The comparison between the PD and LQR controllers, at similar voltage values shows that the LQR produces better results, and in some cases where the system tended towards instability with the PD, the LQR shows stability.

CHAPTER 6

Conclusions

This research is concerned with the application of a piezo electric actuator and sensor in active vibration control of a rotation beam considering a prescribed profile for the angular displacement and employing PD and LQR controls.

A governing equation of motion for a beam was developed using Lagrange's equations and the assumed modes method. The first three modes of vibration are considered here.

Subsequently, the effect of addition of the stiffness and moment of the piezo actuator was observed for three positions of the actuator along the beam's length. The results show, that for the first two modes of vibration, the most effective position for suppressing the tip displacement was the placement of the piezo actuator at the root of the beam. For the second mode of vibration, placement of the piezo actuator in the center or end position, amplifies the displacement of the tip regardless of any positive gain values used with PD control. For the third mode of vibration, when the piezo is placed at the root of the beam, the displacement of the tip was amplified for the PD control. It all cases, the use of the LQR showed that the tip displacement eventually tends to zero. Hence the LQR can be deemed the more effective of the two linear controllers investigated here.

The results for the control vibration may be improved by optimization of the dimensions and the location of the piezo material, and possible using several actuators and sensor in varying configurations. The using of genetic algorithm is a possible path for optimization.

The use of the piezo in layers, which has been investigated in shaped control and low voltage applications, can also be used to improve the results.

The PD and LQR both belong to a class of control referred to as broadband controls. Broadband controls can be susceptible to undesired frequency regions; hence, use of a hybrid control may also serve to improve results.

References

ABREU, G. L., RIBEIRO, J., & STEFFEN JÚNIOR, V. (April de 2003). Experiment on optimal vibration control of a flexible beam containing piezoelectric sensors and actuators. *Shock and Vibration*, pp. 283-300.

DADFARNIA, M., JALILI, N., LIU, Z., & DAWSON, D. M. (2004). An observer-based piezoelectric control of flexible Cartesian robot arms: theory and experiment. *Control Engineering Practice*, 1041-1053.

DJOJODIHARDJO, H., JAFARI, M., WIRIADIDJAJA, S., & AHMAD, K. A. (2015). Active Vibration Suppression of an elastic piezoelectric sensor and actuator fitted cantilevered beam configuration as a generic smart composite structure. *Composite Structures*, 848-863.

FENILI, A.: On Slewing Structure: Modeling and Dynamical Analysis, PHd Thesis presented at State University of Campinas, SP, Brazil (in Portuguese), 2000.

GANI, A., SALAMI-SMIEEE, & KHAN, R. (2003). Active Vibration Control of a Beam with Piezoelectric Patches: Real-time Implementation with xPC target. *Proceedings of 2003 IEEE Conference on Control Applications - CCA*, (pp. 538-544). Istanbul.

HEMMATI, S., SHAHRAVI, M., & MALEKZADEH, K. (2013). Active Vibration Control of Satellite Flexible Structures during Attitude Maneuvers. *Research Journal of Applied Sciences, Engineering and Technology*, pp. 4029-4037.

HU, Q., & MA, G. (April de 2006). Spacecraft Vibration Suppression Using Variable Structure Output Feedback Control and Smart Materials. *Journal of Vibration and Acoustics*, pp. 221-230.

JAFARI, M., & DJOJODIHARDJO, H. (2014). Vibration Control of an Elastic Structure using Piezoelectric Sensor and Actuator with Cantilevered Beam as a Case Study. *Scientific Cooperations International Wokshops on Electrical and Computer Engineering Subfields* (pp. 218-226). Istanbul: kok University.

KUMAR, S., SRIVASTAVA, R., & SRIVASTAVA, R. K. (Jan de 2014). Active Vibration of Smart Piezo Cantilever Beam Using PID Controller. *International Journal of Research in Engineering and Technology*, pp. 392-399.

MOLTER, A., FONSECA, J. S., & BOTTEGA, V. (2009). Simultaneous Piezoelectric Actuator and Sensors Placement Optimization and Sensors Placement Optimization and Optimal Control Design For Flexible Non-Prismatic Beams. *20th international Congress of mechanical Engineering.* Gramado.

NARAYANAN, S., & BALAMURUGAN, V. (2002). Finite element modelling of piezolaminated smart structure for active vibration control with distributed sensors and actuators. *Journal of sound and vibration*, 529-562.
POTA, H. R., & ALBERTS, T. E. (Sep de 1995). Multivariable Transfer Functions for a Slewing Piezoelectric Laminate Beam. *Control* , pp. 352-359.

SALMASI, H., FOTOUHI, R., & NIKIFORUK, P. N. (2008). Vibration Control of a Flexible Link Manipulator Using Smart Structures. *IFAC World Congress*, (pp. 11787-11792). Seoul.
SHUEEI-MUH, L. (November de 2007). PD control of a rotating Smart beam with an elastic root. *Journal of sound and vibration*, pp. 109-124.

YAVARI, A., SARKANI, S., & MOYER JR., T. E. (2000). On application of generalized Function to beam bending problems. *International Journal of Solids Structures*, 5675-5705.
YOUSEFI-KOMA, A. (1997). *Active vibration control of smart structures using piezoelements.* Ottawa: Carleton University. Institute for mechanical and Aerospace Engineering. .

ZHANG, J., HE, L., & WANG, E. (March de 2010). Active Vibration Control of Piezoelectric intelligent Structures, VOL.5, NO. 3, MARCH 2010, Zhang. *Journal of Computers*, pp. 401-409.